

# NATIONAL ADVISORY COMMITTEE FOR AERONAUTICS

TECHNICAL NOTE 3926

EXPERIMENTAL COMPARISON OF SPEED - FUEL-FLOW AND  
SPEED-AREA CONTROLS ON A TURBOJET ENGINE  
FOR SMALL STEP DISTURBANCES

By L. M. Wenzel, C. E. Hart, and R. T. Craig

Lewis Flight Propulsion Laboratory  
Cleveland, Ohio



FOR REFERENCE

Washington

March 1957

**LIBRARY COPY**

MAR 8 1957

LANGLEY AERONAUTICAL LABORATORY  
LIBRARY, NACA  
LANGLEY FIELD, VIRGINIA

NOT TO BE TAKEN FROM THIS ROOM

## NATIONAL ADVISORY COMMITTEE FOR AERONAUTICS

## TECHNICAL NOTE 3926

## EXPERIMENTAL COMPARISON OF SPEED - FUEL-FLOW AND SPEED-AREA

## CONTROLS ON A TURBOJET ENGINE FOR SMALL STEP DISTURBANCES

By L. M. Wenzel, C. E. Hart, and R. T. Craig

## SUMMARY

Optimum proportional-plus-integral control settings for control of engine rotational speed with fuel flow were determined by minimization of integral criteria. The optimum settings thus determined correlated well with analytically predicted optimum settings.

At the optimum control settings, the speed overshoot ratio was 1.28; simulated turbine blade temperature did not overshoot. The optimum control settings were not appreciably altered by the limitation of the rate of change of fuel flow.

The frequency response of engine speed to exhaust-nozzle area could be represented by a linear lag, specified by the rotor time constant, plus a dead time. The linearity of the system, however, is limited to the extent of the physically realizable area change, and thus holds only for small disturbances.

Over a limited range, speed was satisfactorily controlled by exhaust-nozzle area. Within this range, this system was found to possess certain advantages over the speed - fuel-flow control.

## INTRODUCTION

Control of the rotational speed of a turbojet engine is a primary means of regulating thrust and maintaining safe operating limits. Optimization of speed control is therefore of considerable practical importance and has been the object of much endeavor.

Several criteria for use in optimizing closed-loop control systems are suggested in references 1 and 2. In general, these criteria specify optimum control settings when an error function, such as  $\int (\text{error})^2 dt$ , where  $t$  is time, is minimized. In reference 3, a method is developed for analytically determining the optimum control for a linear closed-loop

process based on this criterion. This method is then applied to the specific case of a speed - fuel-flow control on a turbojet engine. For a controlled engine with no constraints on speed or temperature, the analytically determined optimum control was a proportional-plus-integral control (neglecting a small derivative term). The loop gain was equal to the engine-time constant divided by the engine dead time, and the control integral time constant was equal to the engine time constant.

Since the proportional-plus-integral control is in wide use, the indicated relations for the optimum control settings would have great utility provided the relatively simple criteria used for optimization result in satisfactory response of engine speed and temperature. In this report, results of an investigation of engine speed control are presented with emphasis on the relations between the responses of engine variables and the values of two different optimizing criteria. A comparison of the experimentally obtained values for optimum control settings with those determined in reference 3 is also made. This comparison gives an indication of the validity of the analytical results for use as a rule of thumb for determination of the optimum control settings for a proportional-plus-integral control.

In addition to the conventional method of controlling speed by fuel flow, speed may also be controlled by exhaust-nozzle area. It is, of course, recognized that by itself a speed-area control is not feasible. However, considerable attention has been directed toward this system with the idea of using it as one loop of a two-loop control.

In order to build up a background for speed-area control, the response of engine speed to exhaust-nozzle area was obtained. The investigation of the speed-area loop was made on a single-loop basis. Two nonlinear control schemes are presented and discussed, and their performance data are given.

## APPARATUS

### Engine

An axial-flow turbojet engine with annular prevaporizing fuel injectors was run in a sea-level static test stand. The engine was equipped with a variable-area exhaust nozzle, which is shown schematically in figure 1. The electric input signal is converted to a hydraulic signal in the electrohydraulic servomotor. This signal is amplified and converted to rotary motion by the hydraulic power amplifier. The rotary motion thus imparted to the upper vane is transmitted to the lower vane by the interconnecting mechanical linkage.

The frequency response of this system was dependent on the amplitude of the called for change. The response of the area valve to a sinusoidal input for a peak-to-peak amplitude of 15-percent rated area is presented in figure 2.

This variable-area system was designed to have a fast response with little concern about its effect on thrust. As a result, its response is much faster than that of a practical system, and its coefficient of discharge is probably much lower.

### Fuel System

A research-facility fuel valve was used to regulate fuel to the engine manifold. The valve had an amplitude response flat to beyond 10 cycles per second and a dead time of 0.005 second. The description of this valve is given in reference 4.

From the engine manifold the fuel was distributed to flow dividers mounted circumferentially around the engine and finally to the vaporizing fuel injectors.

### Computer

An electronic analog computer was used to perform the mathematical operations necessary to make up the desired control-loop configurations and to obtain the integral criteria.

## INSTRUMENTATION

### Speed

A magnetic pickup was mounted in the compressor case opposite a row of steel compressor rotor blades. The passing of a compressor blade disturbed a magnetic field produced by the pickup and generated an electric pulse at the output terminals.

In order to obtain a transient-speed signal, these pulses were fed to an electronic circuit which produced a voltage proportional to the number of pulses per unit time. No dynamics could be measured in this system within the frequency range of concern. The pulses were also fed to a digital pulse counter to measure steady-state speed.

### Tailpipe Gas Temperature

Transient tailpipe gas temperature was obtained by measuring the output of 16 thermocouples which were distributed around the periphery of the tailpipe. Pairs of the thermocouples were connected in series, and the outputs of the pairs were paralleled. The thermocouples were constructed of 22-gage chromel-alumel wire and had a time constant of approximately

0.30 second at the operating conditions. The output of four similar pairs of thermocouples was connected to a self-balancing potentiometer to read steady-state tailpipe gas temperature.

#### Fuel Flow

A signal indicative of fuel flow during a transient was obtained by measuring the position of the throttle valve in the fuel control by means of a linear differential transformer. It is highly probable that higher-order dynamics were added to the system by the fuel manifold and flow dividers. However, because of the extreme difficulty in measuring actual fuel flow into the engine, the position of the throttle valve was chosen as the signal to be used. If the addition of higher-order dynamics by the distribution system of the engine is neglected, then fuel flow is proportional to throttle-valve position, because the research-facility fuel valve was designed to maintain a constant pressure drop across the throttle valve. Steady-state fuel flow was measured on a rotameter.

#### Exhaust-Nozzle Area

A measure of exhaust-nozzle area was obtained by connecting a position sensor to one of the rotating shafts, as indicated in figure 1. Although the rotation of this shaft is not exactly proportional to exhaust-nozzle area, only small errors result if linearity is assumed.

#### Recorder

A six-channel direct-writing recorder was used to record transient control data. The recorder had a frequency response essentially flat to 100 cycles per second. A galvanometric oscillograph recorder was used to record sinusoidal frequency-response data. The wider range of chart speeds available on this recorder made it more applicable for these purposes. The frequency response of this recorder was essentially flat to beyond 100 cycles per second.

### DYNAMICS, CONTROLS, AND OPTIMIZING CRITERIA

#### Engine Dynamics

Shown in figure 3 is the frequency response of engine rotational speed to exhaust-nozzle area. These data were obtained by sinusoidally varying the exhaust nozzle and measuring the resultant speed fluctuations. The data were taken over the same speed range as was subsequently used in the controls study. The data may be represented by a first-order lag with a time constant of 0.83 second plus a dead time of 0.021 second, as shown by the curves in figure 3.

The response of engine rotational speed to a sinusoidal input to the fuel valve is shown in figure 4. Intuitively, this response should have the same basic time constant as the speed-area response. However, transferring the first-order amplitude response curve from figure 3 to figure 4 shows that additional dynamics are present in this system. These dynamics are attributed to the fuel distribution and combustion processes. (The phase-shift curves drawn in fig. 4 will be discussed in the section "Selection of optimum control settings.") The data of figure 4 were taken over the speed range used in the controls study.

A transient-data trace showing the response of engine variables to a burst in fuel flow is presented in figure 5. The dead time between the input and the beginning of the response of speed is 0.079 second. (Dead time is measured to the break in acceleration because it is more evident than the speed break.)

#### Speed - Fuel-Flow Control

A block diagram of the speed - fuel-flow control loop is presented in figure 6(a). The control is of proportional-plus-integral configuration, and its action may be represented by the transfer function  $K_L \left( 1 + \frac{1}{\tau_{cs}} \right)$ . (Symbols are defined in appendix A.) The loop gain  $K_L$  is defined as the product of the frequency invariant gains of the loop components. Since the gains of all the components except the control are considered constant over the range of test conditions,  $K_L$  will hereinafter be referred to as a control setting.

The operation of the control loop is thus: Measured speed  $N_m$  is compared with set speed  $N_s$ , and the difference, or speed error  $N_e$ , is applied to the input of the control. The error signal is modified according to the control transfer function and fed to the fuel valve. The fuel valve then manipulates fuel flow until  $N_e$  becomes zero.

#### Speed-Area Control

In this investigation, the operating point of the exhaust-nozzle area was close to its wide-open position. Thus, a limited amount of additional area was available for acceleration. When operated as a closed-loop system, the speed-area loop became nonlinear when the control called for more area opening than was physically realizable.

If a linear proportional-plus-integral control were used in this system, adverse effects would occur when the system became nonlinear. At

these conditions, an excessive charge would build up on the integral portion of the control, holding the area wide open after the error had been reduced. This action would cause large speed overshoots. In order to obtain good closed-loop performance, some means was required to prevent this excessive charge from building up while the area was wide open. Two non-linear control schemes were investigated and are described subsequently.

A block diagram of speed-area control type I is presented in figure 6(b). The operation of this control during an acceleration is as follows: Inputs a, b, and c occur simultaneously. Input a initiates a step change,  $\Delta N_g$ ; input b opens the switch, breaking the control loop; and input c supplies a signal to the area valve, causing it to open to its maximum position.

The engine accelerates when the exhaust-nozzle area is wide open. During the acceleration, the switching circuit compares the decreasing  $N_e$  to a predetermined value, set to about 5 percent of the initial error. When  $N_e$  reaches this level, the switching circuit causes the switch to close, returning the engine to normal closed-loop control.

A block diagram of speed-area control type II is presented in figure 6(c). The operation of this system during an acceleration is thus: A step change  $\Delta N_g$  is initiated. The switching circuit compares the control output, or the signal to the area valve, to a preset level corresponding to the limit of the area movement. When the control output exceeds this limit, the switching circuit opens the switch, preventing any further charge from building up on the integrator. The control then has proportional action only. When  $N_e$  decreases to a value such that the control output no longer exceeds this limit, the switching circuit closes the switch, restoring proportional-plus-integral control.

It is emphasized that these controls were designed for step increases in set speed. For use with other inputs, such as decelerations or ramp changes in set speed, it may be necessary to modify the controls.

#### Optimizing Criteria

Desirable properties of a controlled system are speed and stability of response, characterized by overshoot, solution time, time to first zero, and so forth. Unfortunately, speed and stability of response are often in direct conflict with each other.

In a linear closed-loop system, as loop gain is increased to improve the speed of response, overshoot increases and the system becomes more oscillatory. The designer is called upon to make some compromise between these characteristics. The choice of an optimum control would be greatly

simplified if the designer had available a single figure of merit which took all or most of these conflicting characteristics into account. Some function of the error, which would increase as the errors became larger and of longer duration, would be applicable. This function would be minimized for an optimum control.

Several criteria have been suggested for this purpose (refs. 1 and 2), among which are  $\int_0^\infty e^2 dt$ ,  $\int_0^\infty |e| dt$ ,  $\int_0^\infty te^2 dt$ , and  $\int_0^\infty t|e| dt$ . Chosen for this investigation were  $\int_0^\infty e^2 dt$  and  $\int_0^\infty |e| dt$  because of their simplicity and the ease with which they can be mechanized on an analog computer. The controlled system for which these criteria attained minimum values is defined herein as optimum. A block diagram representative of the system used to obtain the values of the criteria is shown in figure 7.

### PROCEDURE

A steady-state map of engine speed against tailpipe gas temperature is presented in figure 8. Accelerations with speed - fuel-flow and speed-area controls are indicated; the initial point for all accelerations is at 94 percent rated speed, and the final point is at 97 percent rated speed.

The testing procedure was the same for all three control loops. The loops (fig. 6) were set up, and step increases in set speed were initiated. Care was taken to maintain both the size and the initial point of all accelerations uniform.

Control action was varied by changing the loop gain and the control integral time constant. The range of loop gains investigated was from a value approaching the point of instability to approximately 10 percent of that value. The control integral time constant was varied from approximately one-half to four times the engine time constant.

### RESULTS AND DISCUSSION

#### Speed - Fuel-Flow Control

Transient data. - Transient data traces are presented in figure 9 for varying values of loop gain and control integral time constant. The response for a low gain control ( $K_L = 1.5$ ) and  $\tau_c = 1.5$  seconds is shown in figure 9(a). The initial increase in fuel flow is only slightly greater than the final value, causing the error to diminish slowly toward zero. This behavior is similar to an uncontrolled system.

Increasing the loop gain to 7.4, as shown in figure 9(b), improves the speed of performance greatly. The speed error rises toward its final



value quickly, reaching it for the first time 0.33 second after the initiation of the step. It then overshoots 31 percent. Tailpipe gas temperature has an overshoot ratio of 3.1. (Performance parameters of overshoot, overshoot ratio, and time to first zero are defined on this figure.)

A further increase in the loop gain to 10.3 gives somewhat faster performance, as shown in figure 9(c). Reduction of the time to first zero to 0.29 second from 0.33 second (fig. 9(b)) is done at the expense of a large speed overshoot ratio, which is now 1.50. Tailpipe-gas-temperature overshoot ratio has also increased and is now 4.0.

Changing  $\tau_c$  to 0.5 second, with a loop gain of 7.4, makes the system more oscillatory. In figure 9(d), the overshoot is 62 percent, twice that of figure 9(b). The time to first zero is 0.31 second, and the temperature overshoot ratio is 4.1.

Increasing  $\tau_c$  to 4.0 seconds at this loop gain has a stabilizing effect on the system, as shown in figure 9(e). The speed overshoot is reduced to 27 percent and the time to first zero is slightly increased to 0.34 second; the temperature overshoot ratio is reduced to 3.0.

Selection of optimum control settings. - A plot of time to first zero against overshoot ratio obtained from these and other data is presented in figure 10. From this curve, which takes into account the portion of the transient only up to the first overshoot, it appears that it would be desirable to operate with very high  $K_L$  and  $\tau_c$ .

If, however, figure 9(e) is examined closely after the initial oscillations have subsided, it is seen that a small error persists for a relatively long time. This type of error is very difficult to evaluate.

The usefulness of the integral criteria is apparent. The choice of the most favorable system would not be an easy one, if it were based on these small differences in performance. Through the use of the integral criteria, the problem is reduced to simply picking a minimum value.

The values of the integral criteria are plotted against speed overshoot ratio in figure 11. The criteria values are large for slow systems having small overshoots, reach a minimum, and then increase again as the system becomes more oscillatory. Both the criteria attain their minimums with a control integral time constant of 1.5 seconds and an overshoot ratio of 1.28. In figure 10, this point on the curve for  $\tau_c = 1.5$  seconds occurs at a loop gain of approximately 7.

If these control settings, chosen by the integral criteria as optimum, are to be compared with the optimum settings indicated in reference 3, the two systems must be similar.

The dynamics of the theoretical system consisted of a linear lag and a dead time. In the response of speed to exhaust-nozzle area (fig. 3), the experimental data fit response curves of a linear lag and a dead time very well.

In the response of speed to fuel flow (fig. 4), this is not so. Because of the additional dynamics present in the fuel distribution and combustion processes, the data do not fit the first-order response curves. The amplitude ratio is attenuated more rapidly than the linear lag transferred from figure 3, and more phase shift (curve A) is exhibited than would be expected from the linear lag plus the dead time measured in figure 5.

In order to interpret the experimental results, this additional attenuation and phase shift should be combined with that due to the linear lag and dead time to form an effective lag and an effective dead time. In evaluating the effective lag, a curve is faired through the data of the upper portion of figure 4 in the region about an amplitude ratio of 0.7. The faired curve intersects the line of 0.707 amplitude ratio at a frequency of 0.15 cycle per second. This gives  $\tau_{e,eff} = \frac{1}{2\pi \times 0.15} = 1.06$  seconds, as compared with  $\tau_e = 0.83$  second measured from the response of speed to area.

The effective dead time is determined by plotting the phase shift that would result from a linear lag with a time constant of 1.06 seconds (curve B, fig. 4). The difference between this curve and the data is due to the effective dead time. The effective dead time is evaluated by adding to curve B the phase shift due to various amounts of dead time. The best possible match is shown as curve C, which is obtained by the addition of a dead time of 0.15 second. This value of  $t_{d,eff} = 0.15$  second is considerably larger than the value for dead time measured from figure 5, which is 0.079 second.

According to reference 3, the optimum control settings are  $\tau_{c,opt} = \tau_e$ , and  $K_L = \tau_e/t_d$ . Applying these relations to this system gives  $\tau_{c,opt} = \tau_{e,eff} = 1.06$  seconds, and  $K_{L,opt} = \frac{\tau_{e,eff}}{t_{d,eff}} = 7.1$ . These values compare favorably with those obtained experimentally, which were  $\tau_{c,opt} = 1.5$  seconds and  $K_{L,opt} = 7$ .

Temperature overshoot. - The overshoot ratio of tailpipe gas temperature  $T$  is plotted against speed overshoot ratio in figure 12. For the optimum control settings, the  $T$  overshoot ratio is about 3.0. This temperature was sensed by a thermocouple having a time constant of 0.3 second.

Because of the large  $T$  overshoots obtained, an investigation of the excursions of turbine blade temperature  $T_b$  was made. In order to simulate  $T_b$ , the  $T$  signal was compensated to eliminate the lag of the sensing thermocouple and was then passed through a lag of 1.5 seconds, which is conservatively small for simulation of turbine blade dynamics (ref. 5). A data trace showing the transient behavior of this variable, for a repeat run of the transient shown in figure 9(b), is presented in figure 13.

The turbine-blade-temperature overshoot ratios, obtained with various  $K_L$ 's at  $\tau_c = 1.5$  seconds, are plotted in figure 12. It is seen that at the optimum control settings ( $K_L = 7.4$ ,  $\tau_c = 1.5$ ) no  $T_b$  overshoot occurs. This is important in that a compromise in optimum speed control, for the purpose of limiting temperature excursions, is apparently not required.

Limitation of fuel-valve response. - In order to obtain data more representative of a practical control system, a circuit was added between the control and the fuel valve which limited the rate of change of the signal to the fuel valve. Thus, the rate of change of fuel flow was limited to approximately 150 percent of rated flow per  $10^{\text{th}}$  second.

Transient-data traces for this system are presented in figure 14 for  $K_L$ 's and  $\tau_c$ 's comparable with those in figure 9. Of particular interest in these data is the fuel-valve position trace, which rises on a ramp initially. (This is not clear in fig. 14(a) because the change in fuel flow is small.) Comparison of the traces of fuel-valve position and control output (recorded before the rate-of-change limiting circuit) shows that the fuel valve cannot follow the initial rise but follows the slower return exactly. This action is typical of a motor-driven fuel valve.

The primary effect that the addition of this circuit had on the performance of the system was the increase of time to first zero (fig. 15). This increase was, on the average, about 15 percent for a given set of control constants.

The integral criteria, plotted in figure 16, minimize at higher values than were obtained without the limitation on the fuel-valve response. The minimum values occur at  $\tau_c = 2.0$  seconds and an overshoot ratio of about 1.28. On figure 15, this point corresponds to a loop gain of about 6.5. It is important to note that the control settings necessary to obtain the minimum integral values remain essentially unchanged although the response of the fuel valve has been limited.

The tailpipe-gas-temperature overshoot ratio for this system is plotted in figure 17. For the optimum control settings, the overshoot ratio is about 3.2. Although simulated turbine blade temperatures were not investigated for this system, it may be assumed that no overshoot occurred, since the tailpipe-gas-temperature overshoot ratio is approximately the same.

## Speed - Exhaust-Nozzle-Area Control

The increasing use of afterburners on modern turbojet engines has emphasized the need for two-loop controls in which both speed and tailpipe temperature are controlled. One of the possible two-loop configurations is that in which speed is controlled by exhaust-nozzle area and temperature, by fuel flow.

It is realized that the speed-area control has a limited utility as a single-loop system. However, an investigation was carried out on this basis to avoid the complications that would be caused by a simultaneous manipulation of fuel flow.

Transient data, type I control. - Transient-data traces for speed-area control type I are presented in figure 18 for varying values of  $K_L$  and  $\tau_c$ . Engine response for control settings of  $\tau_c = 0.1$  second and  $K_L = 7.5$  is shown in figure 18(a). Speed overshoots 24 percent, and its time to first zero is about 0.75 second. Since the area is opened to accelerate the engine, tailpipe gas temperature decreases; and the possibility of engine damage due to temperature overshoots is eliminated.

Increasing the gain to 17.5, as shown in figure 18(b), reduces the speed overshoot to 10 percent. The time to first zero is unchanged (0.75 sec). Increasing  $\tau_c$  to 0.5 second (fig. 18(c)) increases the speed overshoot to 22 percent. The time to first zero is again 0.75 second.

The reason for these minute differences in time to first zero is clear. As seen in figure 18, almost all the acceleration is accomplished with the area wide open. Since control action does not begin until the error approaches zero, the initial portion of the speed response is, for all practical purposes, independent of control settings.

Selection of control settings, type I control. - In figure 19 are plotted values of speed overshoot ratio against loop gain. Overshoot ratio is seen to decrease as  $K_L$  becomes larger and  $\tau_c$  becomes smaller. Past a loop gain of about 25, however, only small improvements are realized for further increases of loop gain. Also, amplification of noise increases, and the area tends to follow these unwanted signals. In view of these facts, it is deemed undesirable to operate with a loop gain greater than about 18.

In this system, the primary function of the control is to supply a signal to close the area from wide-open position to its new operating point. This should be done as quickly as possible in order to minimize overshoots. As anticipated, the test data show that a low  $\tau_c$  and a high  $K_L$  would best accomplish this.

4161

CW-2 back

The integral criteria, plotted in figure 20, follow the same trends as does speed overshoot ratio. These trends indicate that the best operation is obtained by using a control having a large  $K_L$  and a small  $\tau_c$ .

Transient data, type II control. - Transient-data traces for speed-area control type II are presented in figure 21 for varying values of  $\tau_c$ . Engine response for control settings of  $\tau_c = 0.1$  second and  $K_L = 7.5$  is shown in figure 21(a). The speed overshoot ratio is 1.20, and the time to first zero is about 0.78 second.

Increasing  $\tau_c$  to 0.5 second (fig. 21(b)) reduces the speed overshoot to a very small value, about 3 percent. The time to first zero has increased to 0.92 second. For this system, the area is not held open as long as it was in figure 21(a).

A further increase in  $\tau_c$  to 1.0 second (fig. 21(c)) results in an overdamped response having no overshoot. The area here remains open for a still shorter time. It is seen in these data that the performance of the system is more dependent on  $\tau_c$  than the system with type I control.

As  $\tau_c$  is decreased, the contribution of the integral term becomes of greater significance. If  $\tau_c$  is too small, as in figure 21(a), a large charge is built up on the integral before the error reaches zero. Since this charge holds the area open after the error has reached zero, the engine continues to accelerate, causing a speed overshoot.

If, on the other hand,  $\tau_c$  is made too large, the response such as shown in figure 21(c) results. The rate at which the integral charges is reduced. Hence, unless  $K_L$  is increased, a sustained error is necessary to build up the integral charge required for operation at the new conditions.

Selection of control settings, type II control. - Speed overshoot ratio is plotted against  $K_L$  in figure 22. It is seen that overshoot may be reduced by increasing  $K_L$  or  $\tau_c$ . In figure 23, values of the integral criterion are constant beyond a  $K_L$  of 7.5 and practically independent of  $\tau_c$ . If similar performance can be obtained by operating at a high or low value of  $K_L$ , it is more desirable to operate at the lower value because of the noise amplification previously mentioned.

In view of these facts, the recommended control settings for this control are  $\tau_c = 0.5$  and  $K_L = 7.5$ . However, since the performance of the system is dependent on the response of the area servomotor and the physical limit of the area opening, this recommendation cannot be generalized.

### Comparison of Speed - Fuel-Flow and Speed-Area Controls

Overtemperature. - As pointed out previously, the trend toward turbine blade damage due to high engine temperatures during an acceleration is not present in the speed-area control.

Speed overshoot. - Speed overshoot for the optimum speed - fuel-flow control is 28 percent. The best operation of the speed-area control is with little or no overshoot.

Acceleration capabilities. - The additional exhaust-nozzle area available for acceleration above the operating point was 13 percent rated area; the additional fuel flow available for acceleration above the operating point was approximately 100 percent rated fuel flow. Therefore, the acceleration capabilities of the speed - fuel-flow control are greater than those of the speed-area control.

Time to first zero. - Because of the larger acceleration capabilities of the speed - fuel-flow control, the time to first zero for this system is smaller.

Solution time. - Because of the speed overshoot obtained with the speed - fuel-flow control, the time required for  $N_e$  to reach and stay within 10 percent of its initial value is about the same for both controls.

Integral criteria. - The values of the integral criteria at their minimums are about the same for both controls.

Dependence on control settings. - The control integral time constant and the loop gain must be held to close tolerances for optimum operation with the speed - fuel-flow control but considerable variation is allowable for the speed-area systems.

Simplicity of control. - The presence of the limit in the area necessitated the use of a nonlinear speed-area control, which involved additional circuitry. Since the speed - fuel-flow loop was linear, the control was simple in comparison.

The comparisons between the two systems are summarized in the following table. In this table, + denotes more favorable action; -, less favorable action; and o, similar action by both systems.

	Speed - fuel-flow control	Speed-area control
Overtemperature	-	+
Speed overshoot	-	+
Acceleration capabilities	+	-
Time to first zero	+	-
Solution time	o	o
Integral criteria	o	o
Dependence on control settings	-	+
Simplicity of control	+	-

### CONCLUSIONS

The optimum speed - fuel-flow control obtained in this investigation, based on minimization of error integral criteria, can be satisfactorily predicted by application of linear theory. Agreement was good, although higher-order dynamics were present in the engine that were not considered in the linear analysis. The theoretical optimum control is of proportional-plus-integral configuration, and its action may be represented by the transfer function  $K_L \left( 1 + \frac{1}{\tau_c s} \right)$ . The loop gain  $K_L$  is equal to the ratio of the engine time constant to the engine dead time, and the control integral time constant  $\tau_c$  is equal to the engine time constant;  $s$  is the Laplace operator.

At the optimum control settings, the speed overshoot ratio was 1.28. Simulated turbine blade temperature did not overshoot, indicating a compromise in optimum speed control, for the purpose of limiting temperature excursions, is apparently not required. Limitation of the rate of change of fuel flow did not appreciably alter the values of the optimum control settings.

The frequency response of engine speed to exhaust-nozzle area could be represented by a linear lag, specified by the rotor time constant, plus a dead time. The linearity of the system, however, is limited to the extent of the physically realizable area change and thus holds only for small disturbances.

When used as a controlling variable, the area is frequently opened to its maximum position. If a proportional-plus-integral control is to be used in the speed-area loop, some provision must be made to prevent saturation of the integral component of the control while the area is on its limit.

By using a nonlinear control with this characteristic, speed was satisfactorily controlled by exhaust-nozzle area over a limited range. Within this range, the speed-area loop was found to possess advantages over the speed - fuel-flow loop with respect to speed and temperature overshoots.

Lewis Flight Propulsion Laboratory  
National Advisory Committee for Aeronautics  
Cleveland, Ohio, December 13, 1956



## APPENDIX A

## SYMBOLS

a,b	constants associated with integral criteria
e	error
$K_L$	loop gain
N	engine rotational speed, percent rated
s	Laplace operator
T	tailpipe gas temperature, percent rated
t	time, sec
$t_d$	dead time, sec
$w_f$	fuel flow, percent rated

## Subscripts:

b	turbine blade
c	control
e	error
eff	effective
m	measured
opt	optimum
s	set

## REFERENCES

1. Hall, Albert C.: The Analysis and Synthesis of Linear Servomechanisms. The Technology Press, M.I.T., Cambridge (Mass.), 1943.
2. Graham, Frank D., and Lathrop, Richard C.: Synthesis of "Optimum" Transient Response - Criteria and Standard Forms. WADC Tech. Rep. No. 53-66, Wright Air Dev. Center, Air Res. and Dev. Command, Wright-Patterson Air Force Base, Aug. 1953. (RDO No. 206-11.)

3. Boksenbom, Aaron S., Novik, David, and Heppler, Herbert: Optimum Controllers for Linear Closed-Loop Systems. NACA TN 2939, 1953.
4. Otto, Edward W., Gold, Harold, and Hiller, Kirby W.: Design and Performance of Throttle-Type Fuel Controls for Engine Dynamic Studies. NACA TN 3445, 1955.
5. Hood, Richard, and Phillips, William E., Jr.: Dynamic Response of Turbine-Blade Temperature to Exhaust-Gas Temperature for Gas-Turbine Engines. NACA RM E52A14, 1952.

Total

CW-3

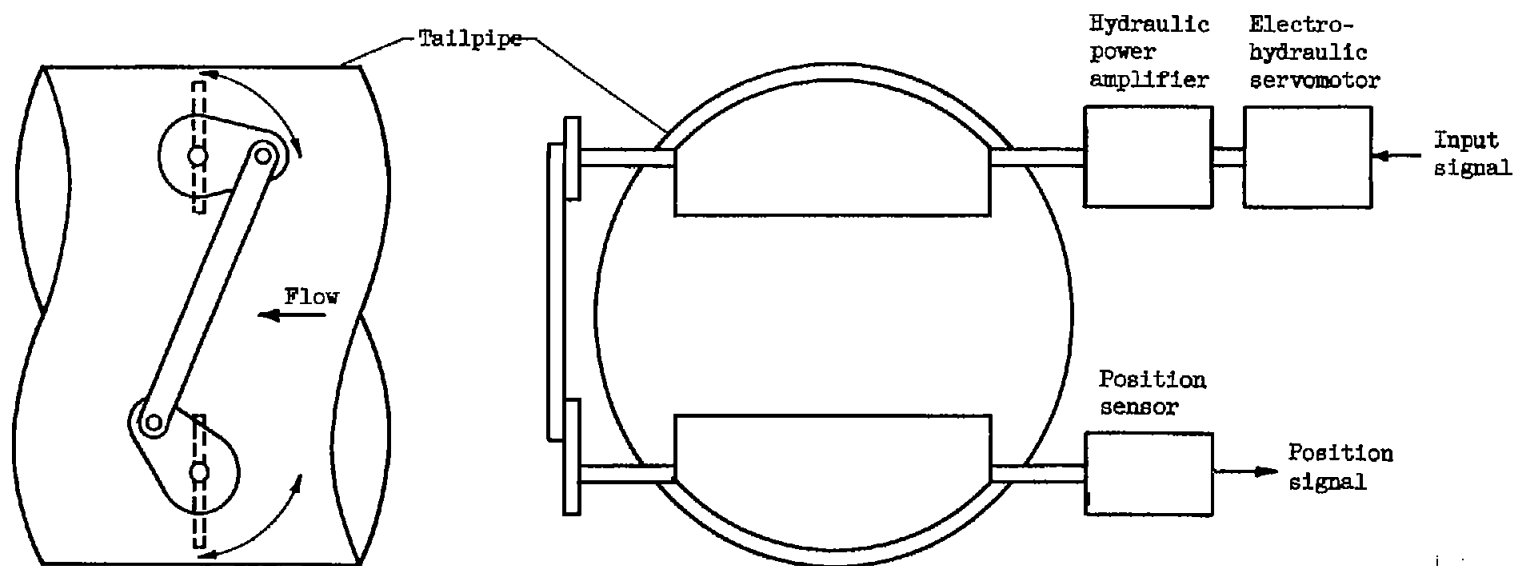


Figure 1. - Schematic diagram of variable-area exhaust-nozzle system.

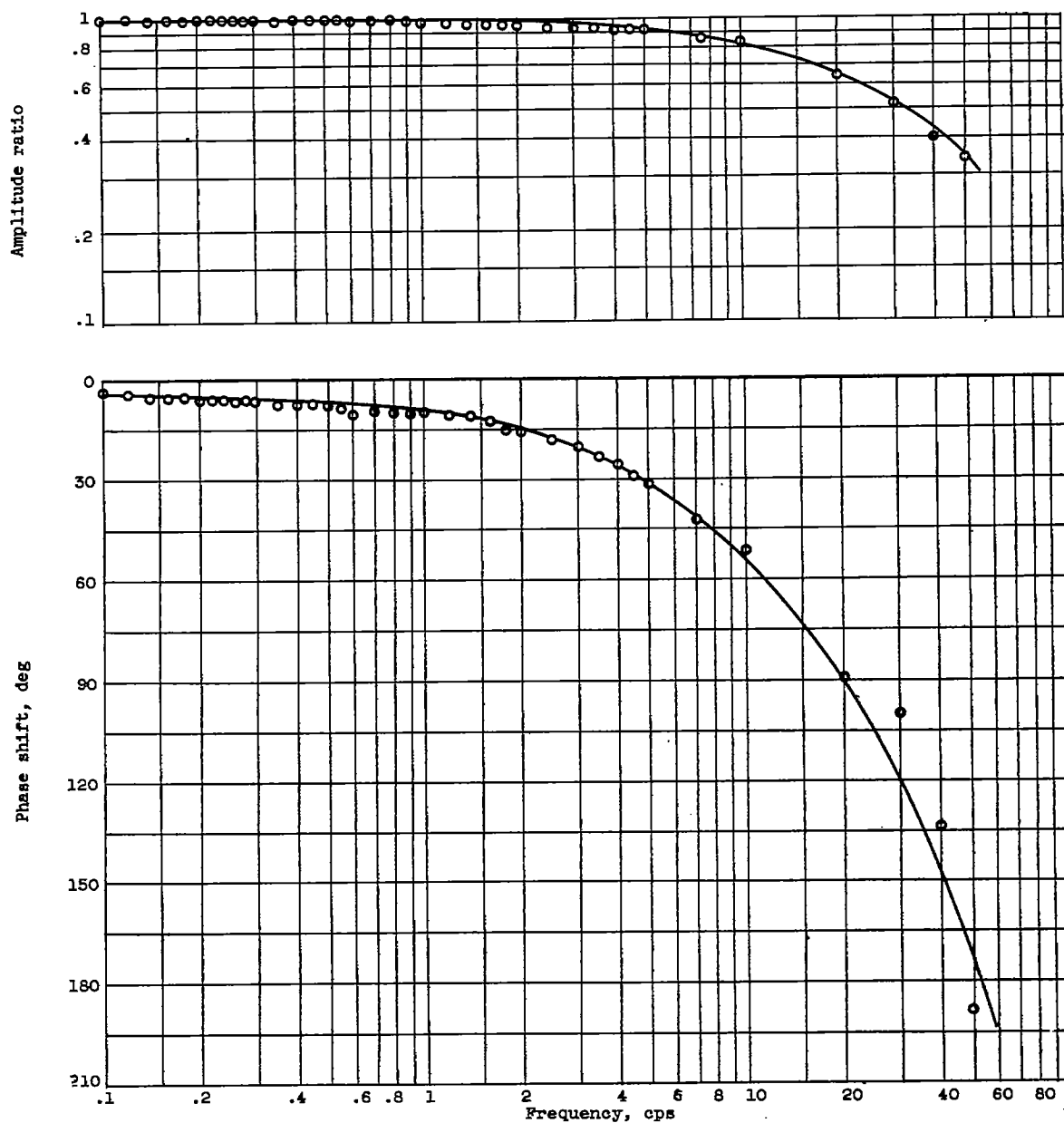


Figure 2. - Frequency response of exhaust-nozzle position to sinusoidal input of  $\pm 5$ -percent rated area.

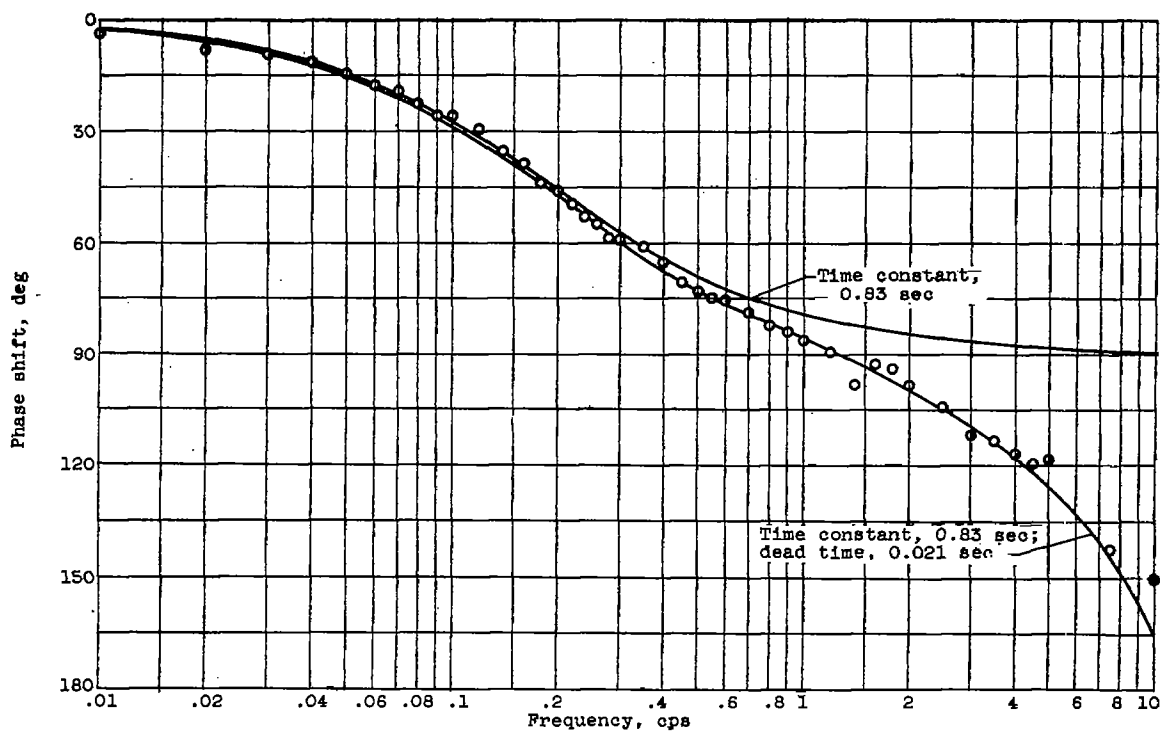
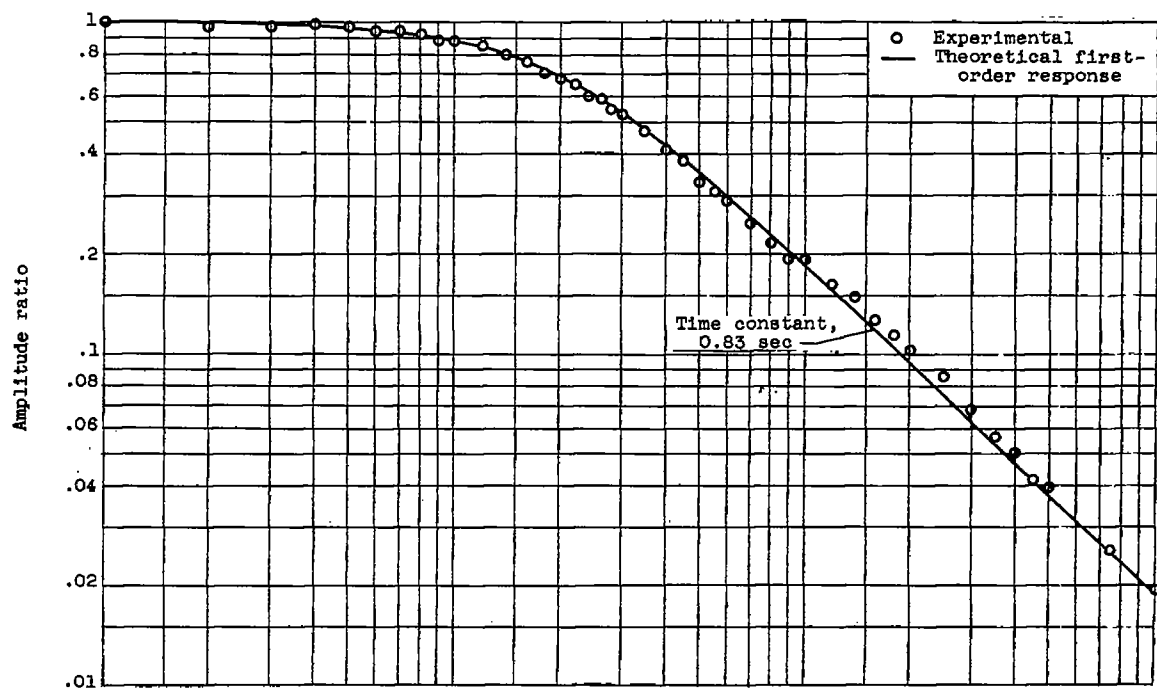


Figure 3. - Frequency response of engine rotational speed to sinusoidal variation of exhaust-nozzle position. Operating range,  $95.5 \pm 3$  percent rated speed.

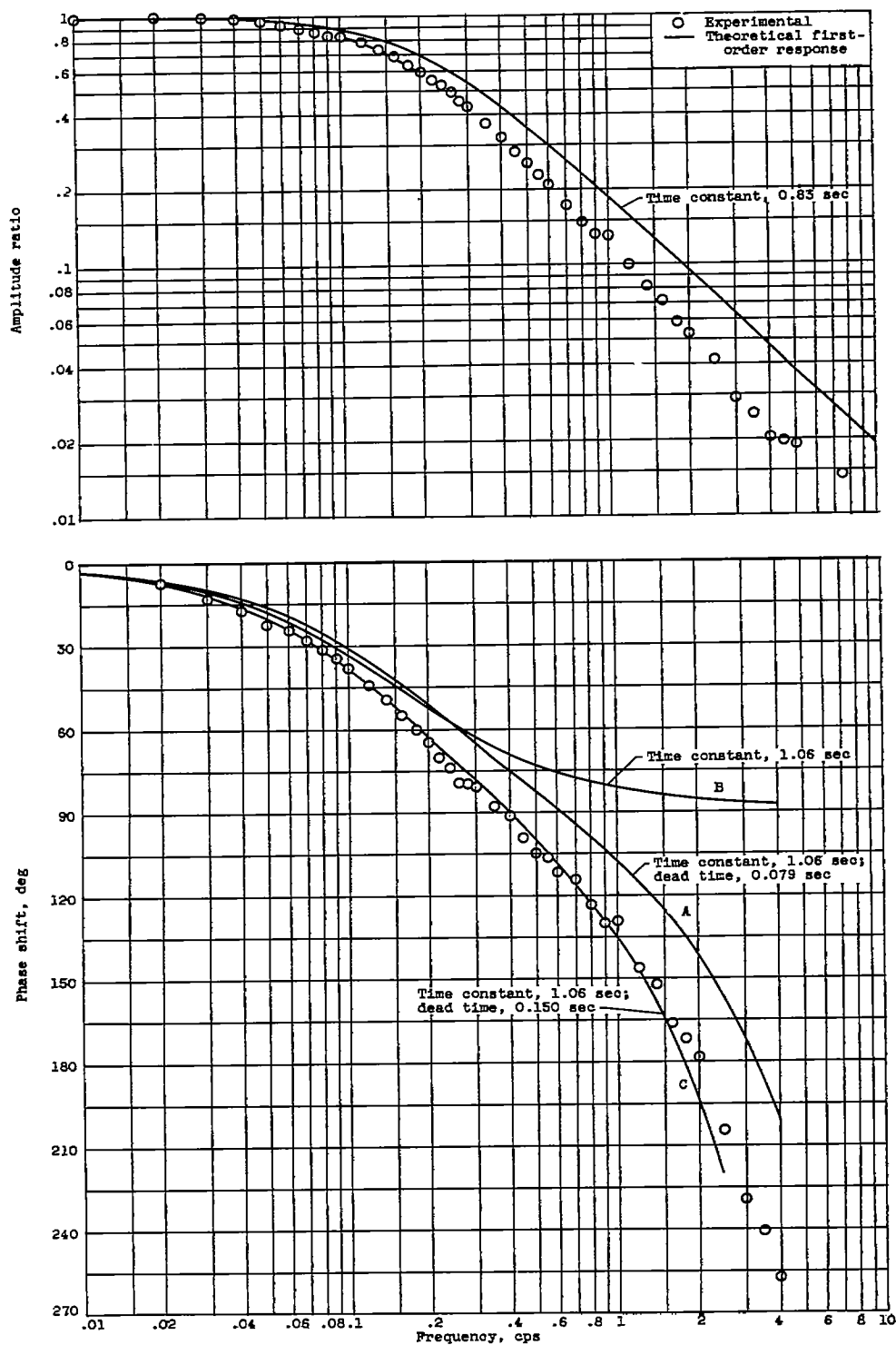


Figure 4. - Frequency response of engine rotational speed to sinusoidal input to fuel valve. Operating range, 95.5±3 percent rated speed.

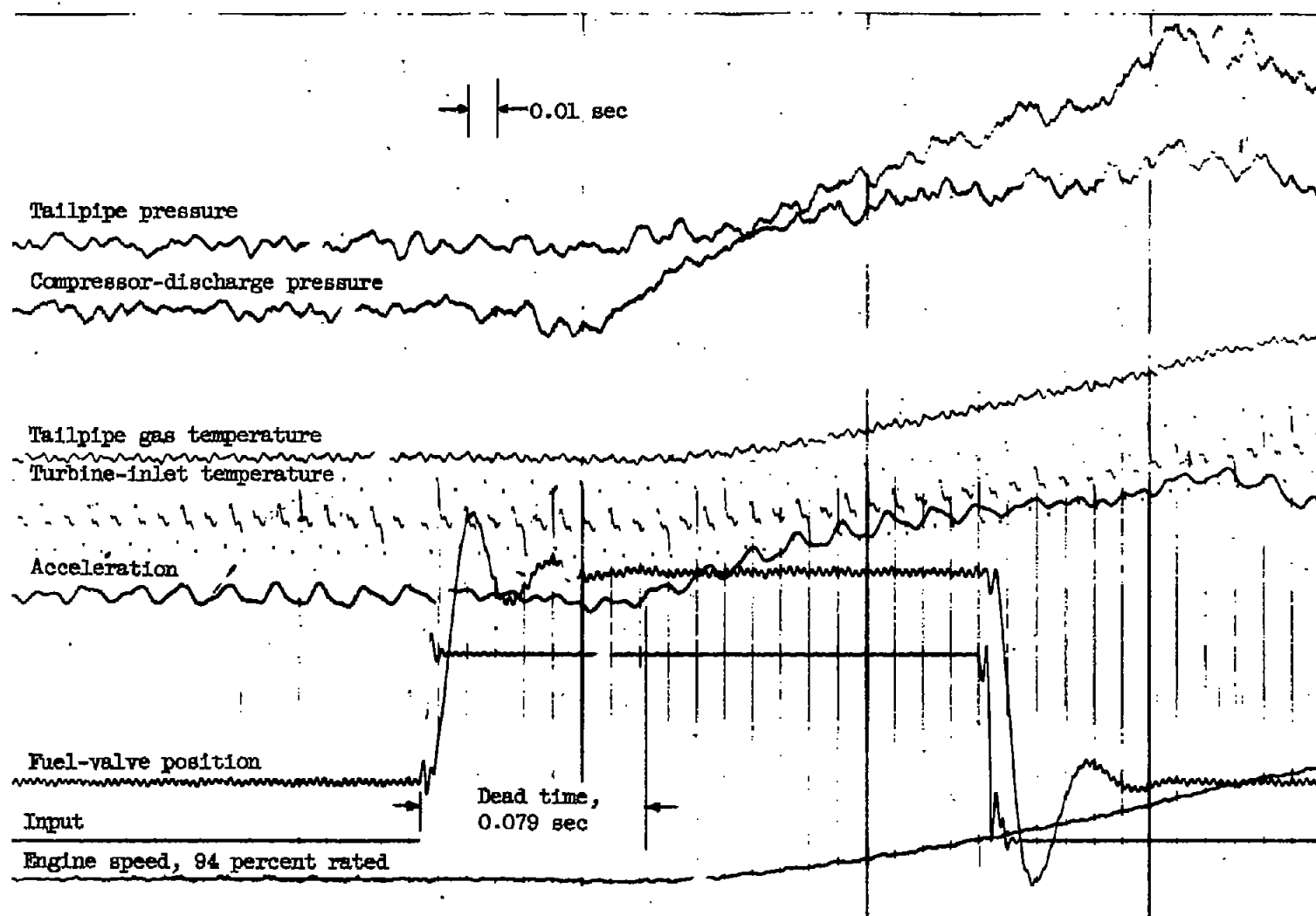
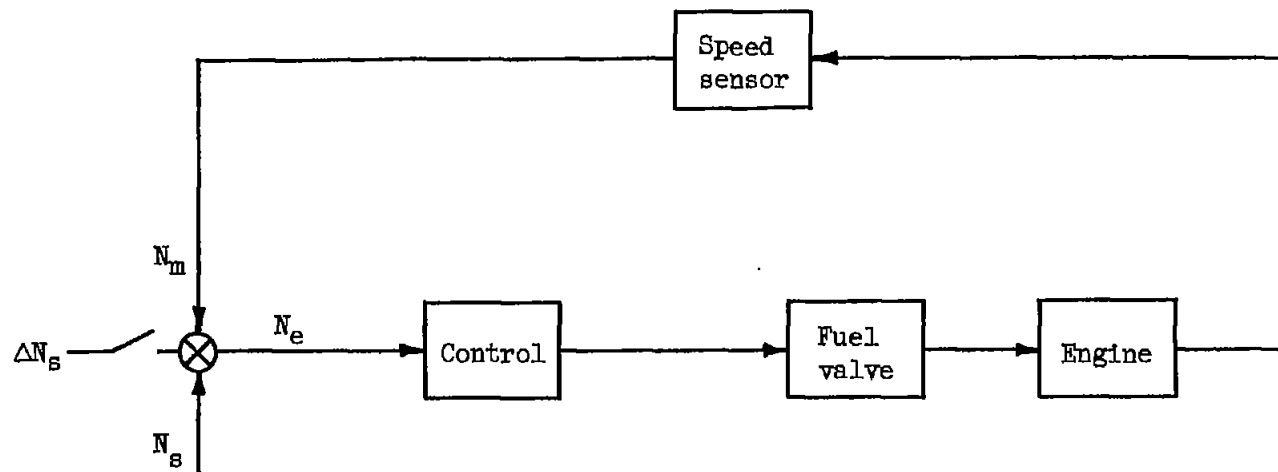


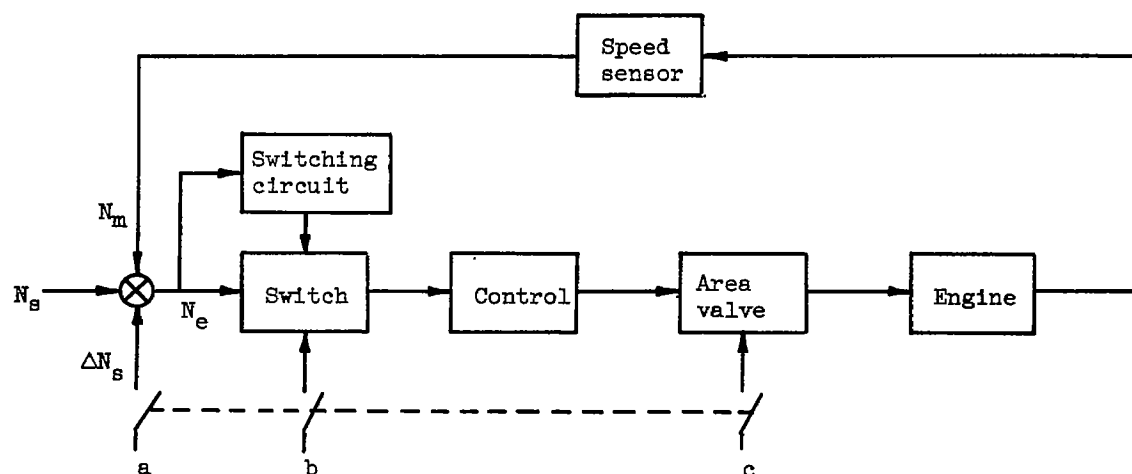
Figure 5. - Response of uncontrolled engine to burst in fuel flow illustrating dead time present.



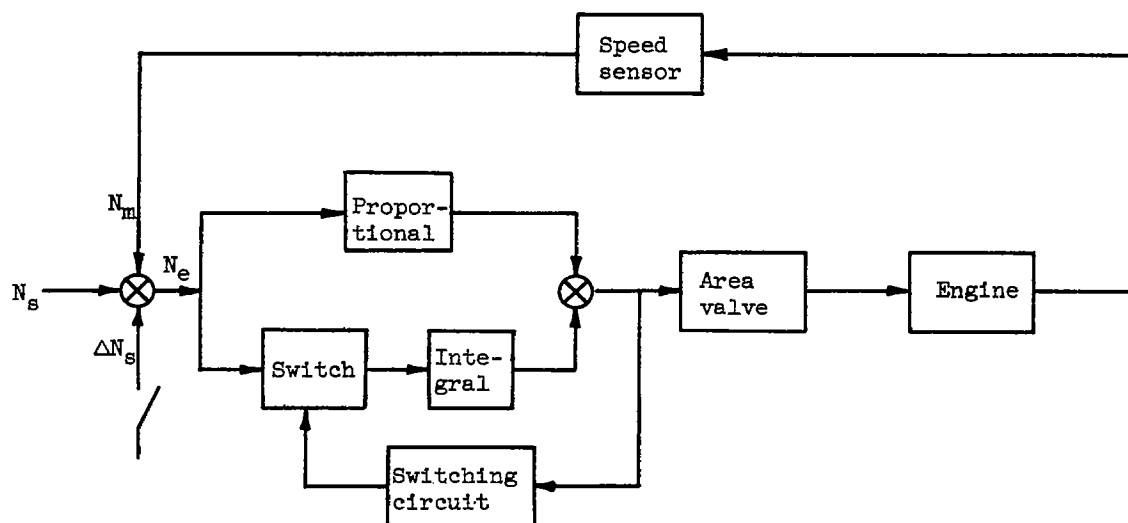
(a) Speed - fuel-flow control.

Figure 6. - Block diagram of control loops.





(b) Speed-area control type I.



(c) Speed-area control type II.

Figure 6. - Concluded. Block diagram of control loops.

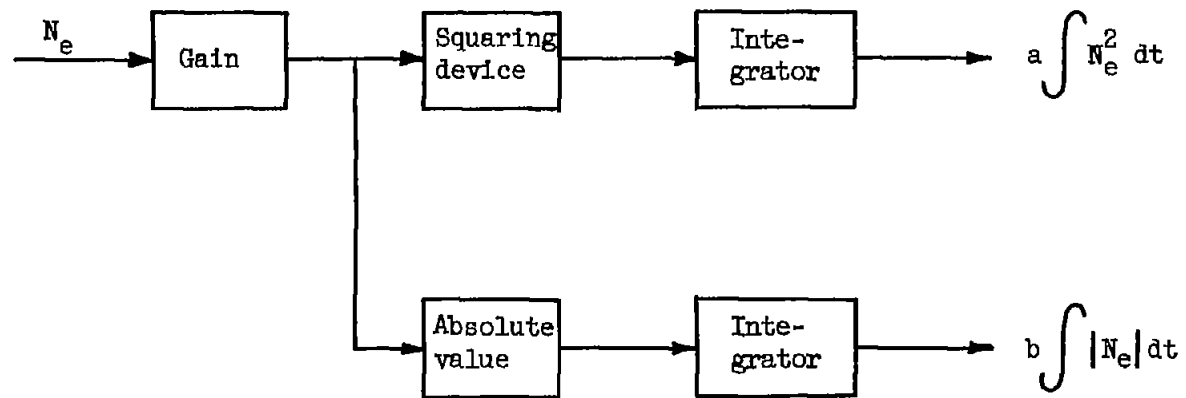


Figure 7. - Block diagram of system used for obtaining integral criteria.

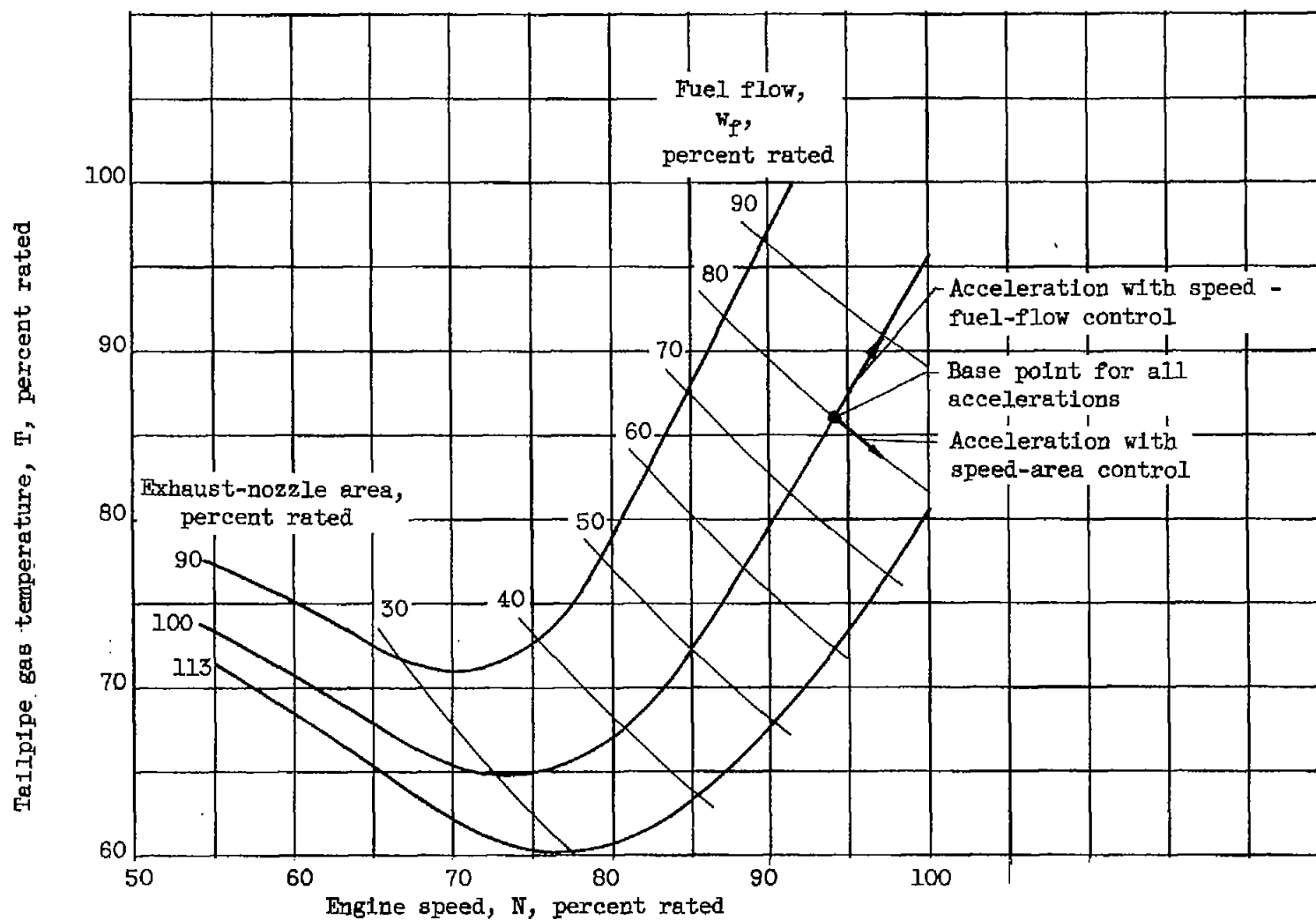
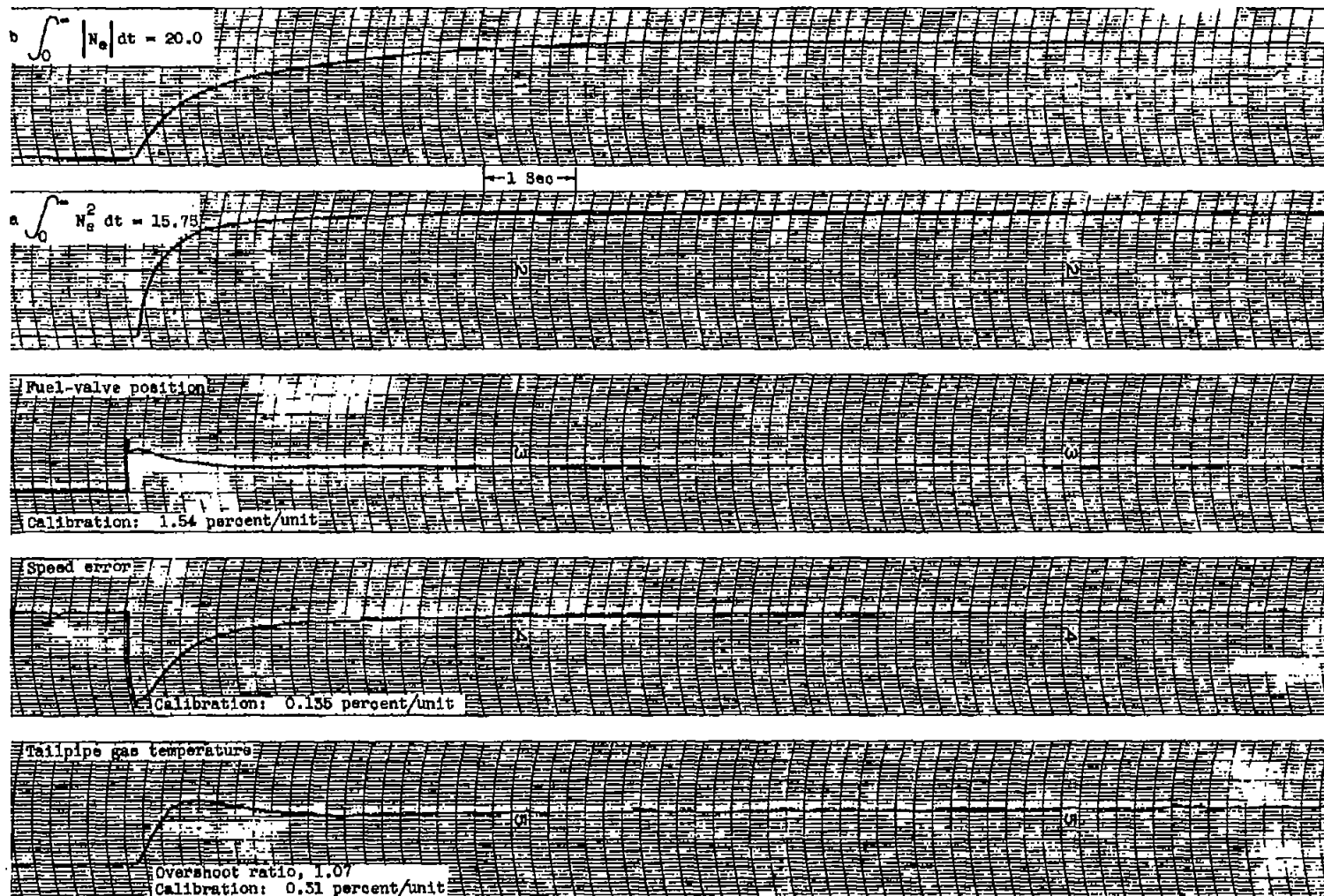
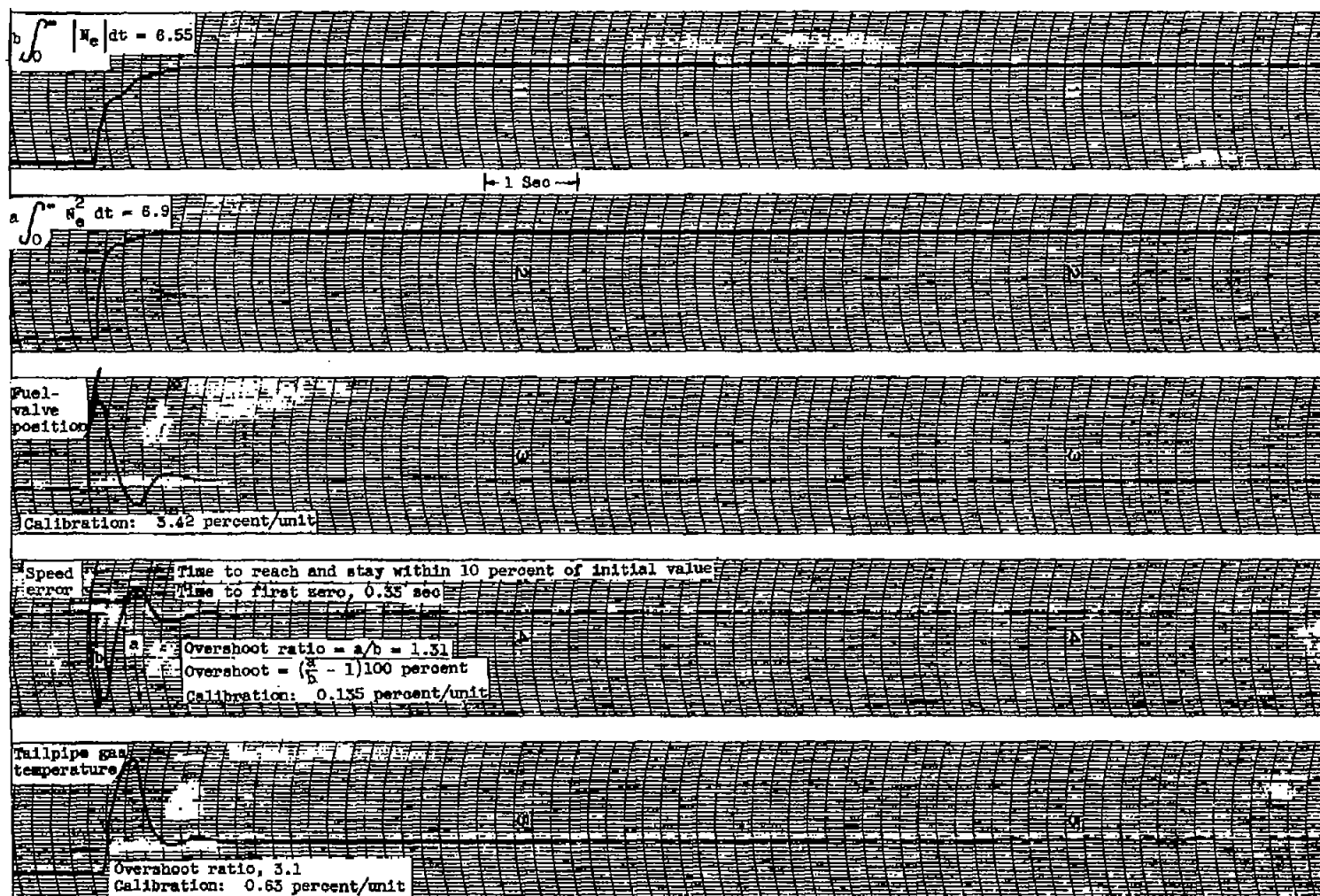


Figure 8. - Steady-state map of engine variables.



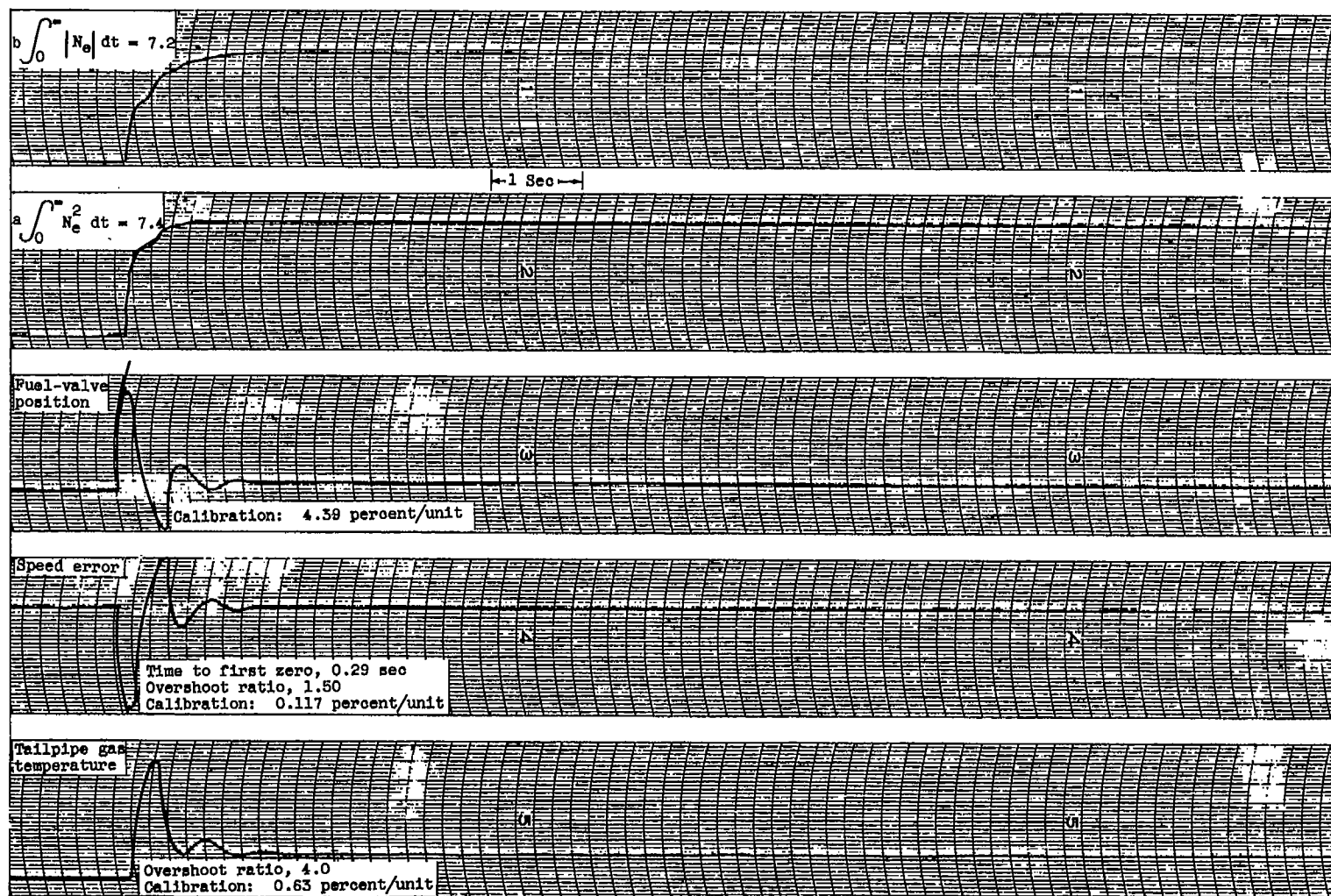
(a) Control integral time constant, 1.5 seconds; loop gain, 1.5.

Figure 9. - Transient data for speed - fuel-flow control for step increase in engine set speed.



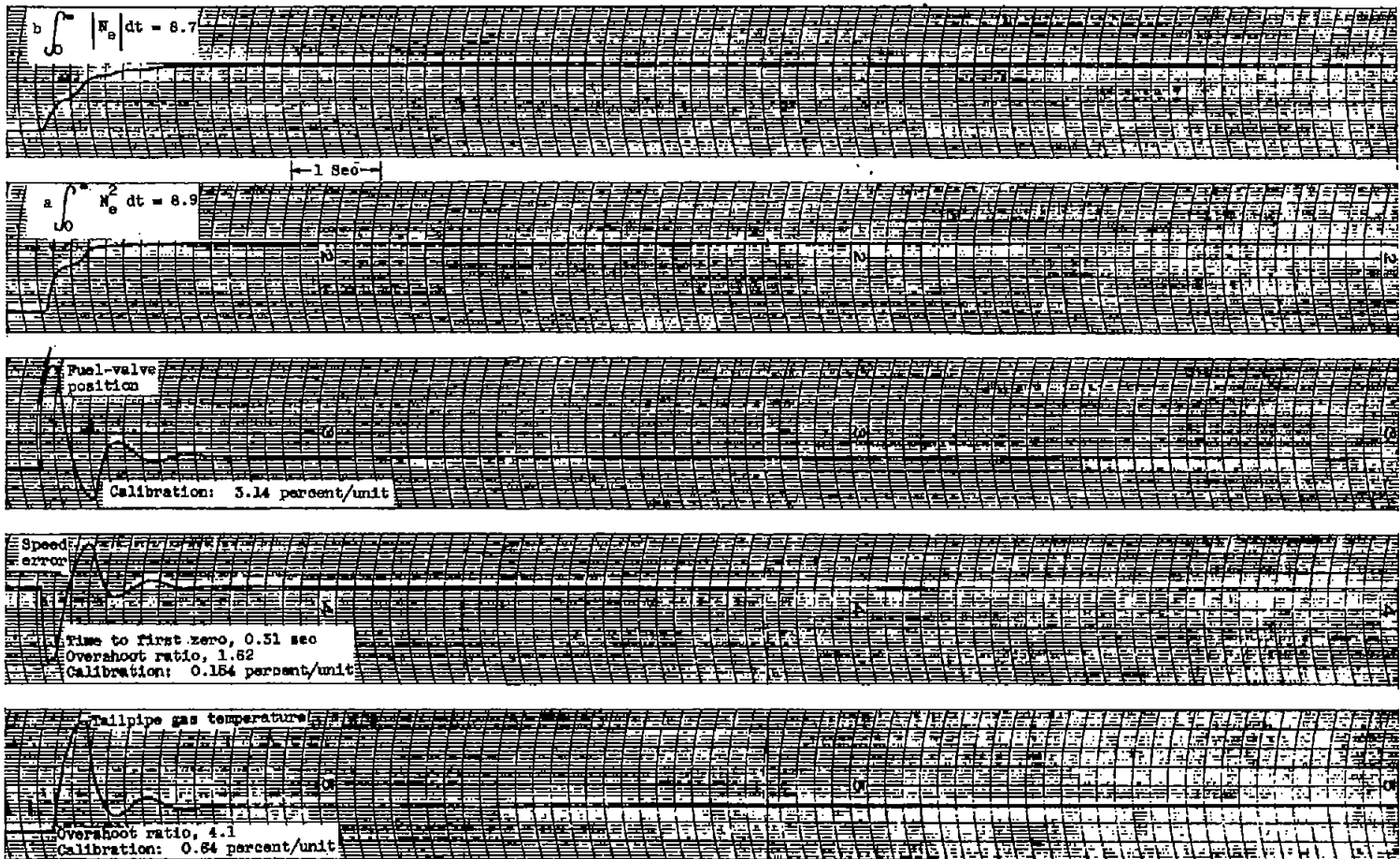
(b) Control integral time constant, 1.5 seconds; loop gain, 7.4.

Figure 9. - Continued. Transient data for speed - fuel-flow control for step increase in engine set speed.



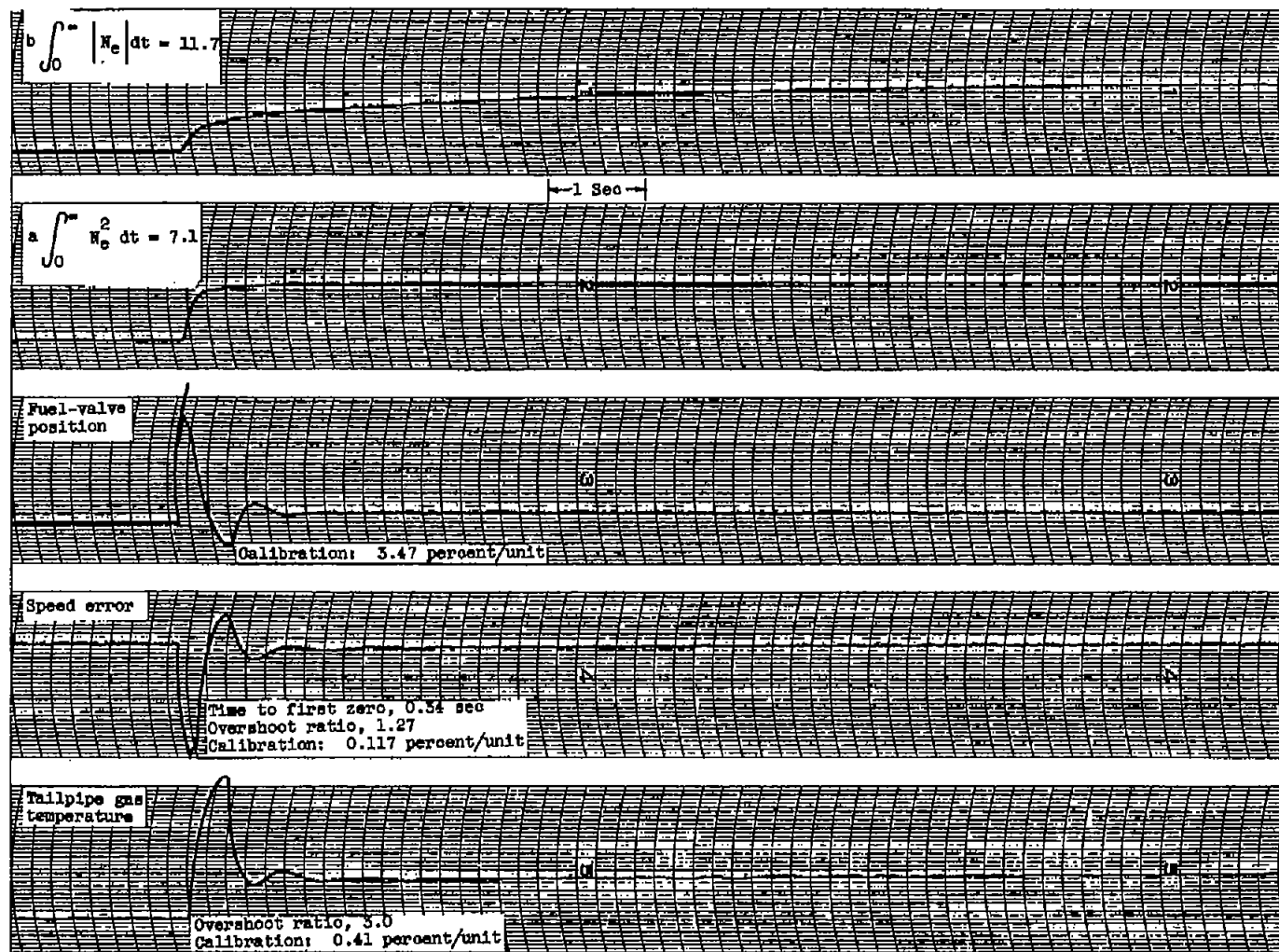
(c) Control integral time constant, 1.5 seconds; loop gain, 10.3.

Figure 9. - Continued. Transient data for speed - fuel-flow control for step increase in engine set speed.



(d) Control integral time constant, 0.5 second; loop gain, 7.4.

Figure 9. - Continued. Transient data for speed - fuel-flow control for step increase in engine set speed.



(e) Control integral time constant, 4.0 seconds; loop gain 7.4.

Figure 9. - Concluded. Transient data for speed - fuel-flow control for step increase in engine set speed.



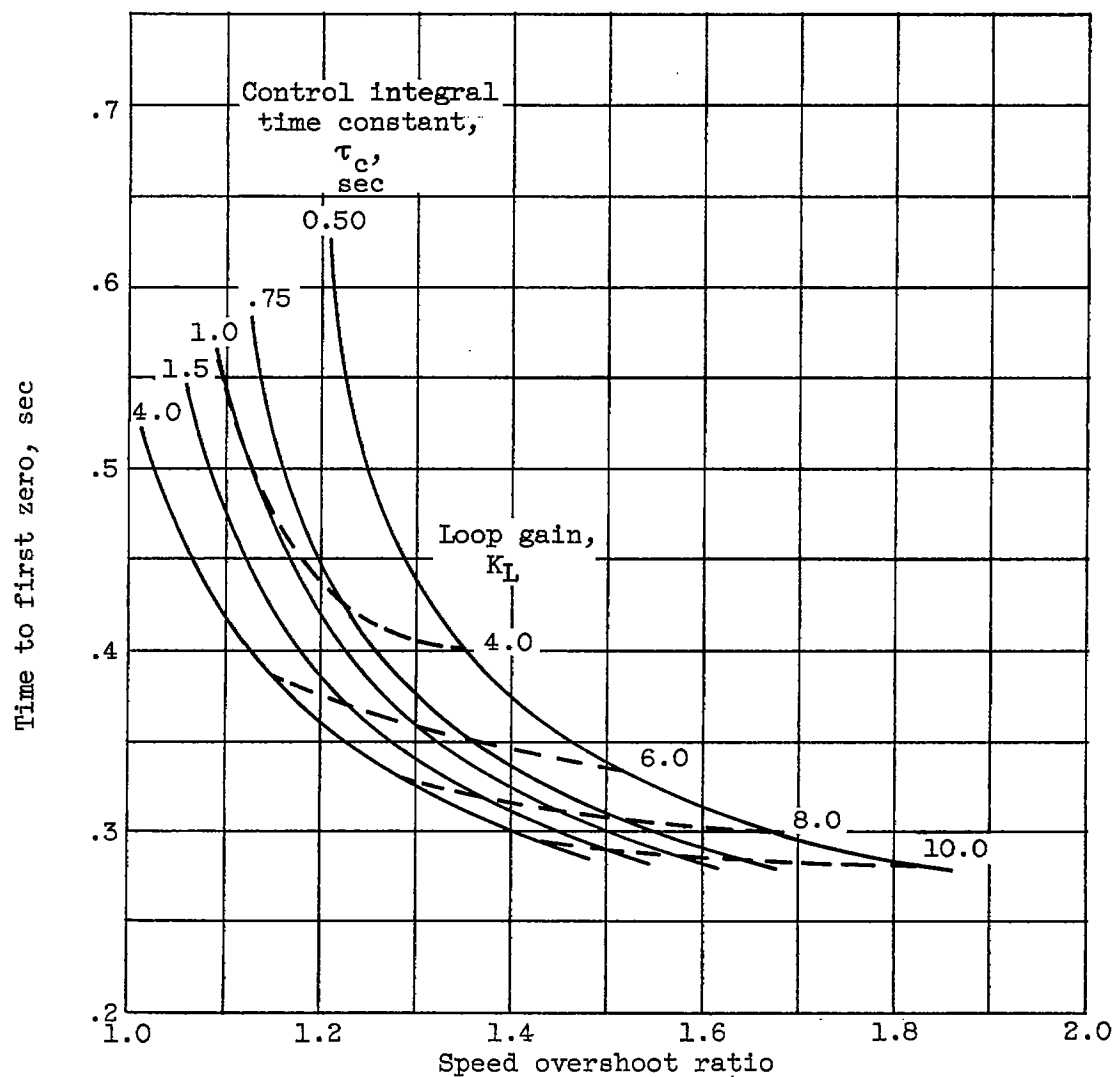


Figure 10. - Variation of time to first zero with speed overshoot ratio for speed - fuel-flow control.

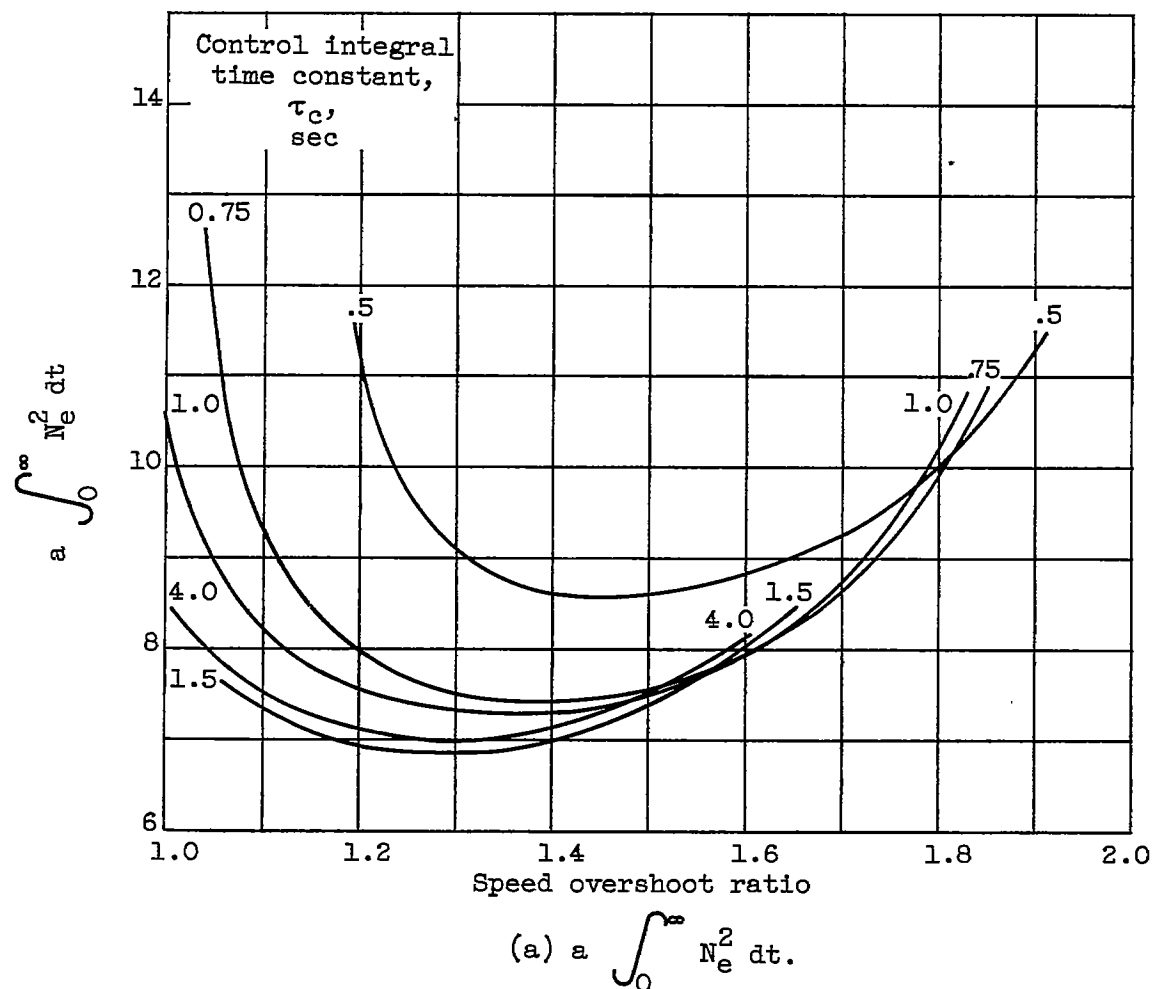


Figure 11. - Variation of integral criteria with speed overshoot ratio for speed - fuel-flow control.

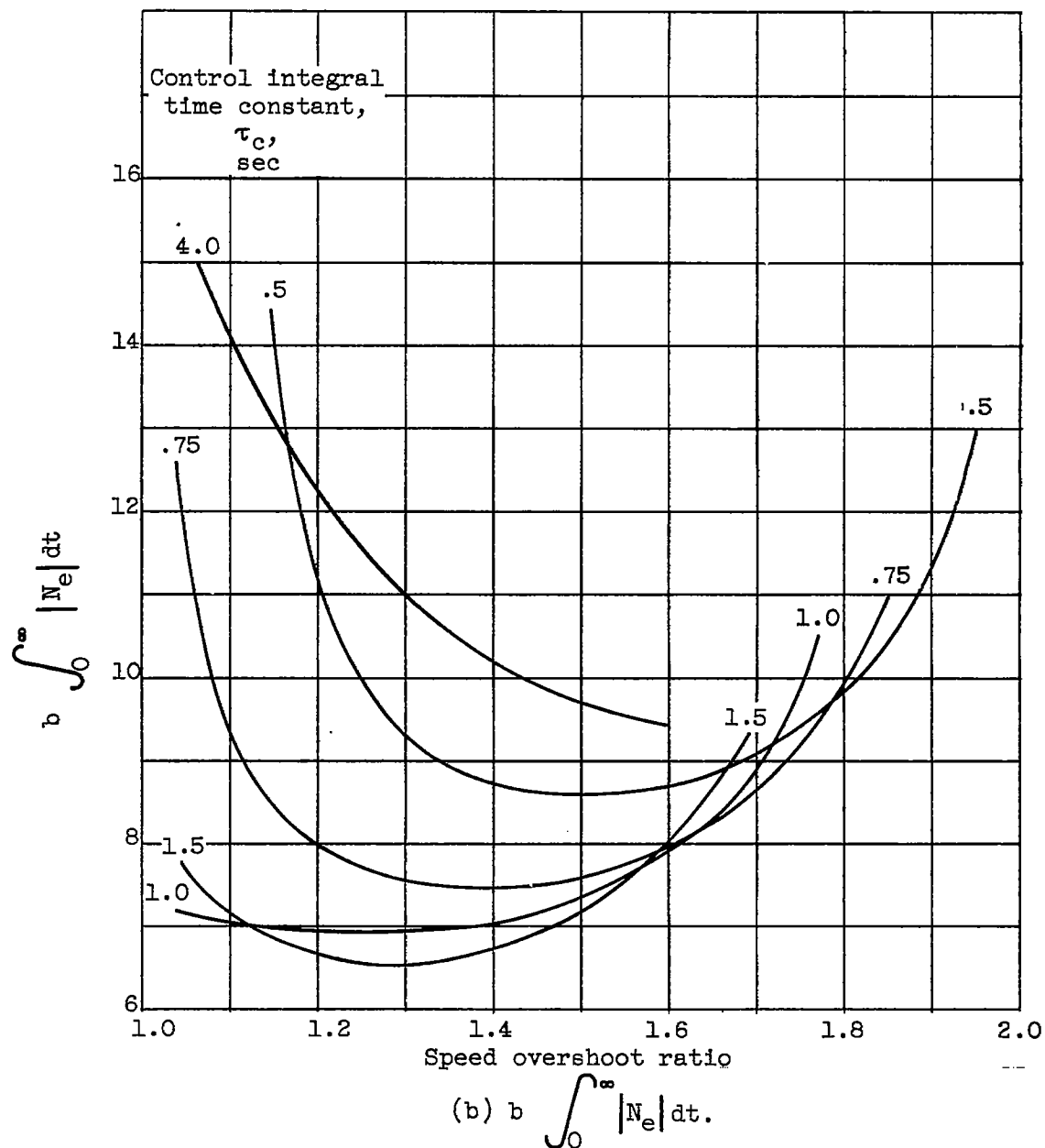


Figure 11. - Concluded. Variation of integral criteria with speed overshoot ratio for speed - fuel-flow control.

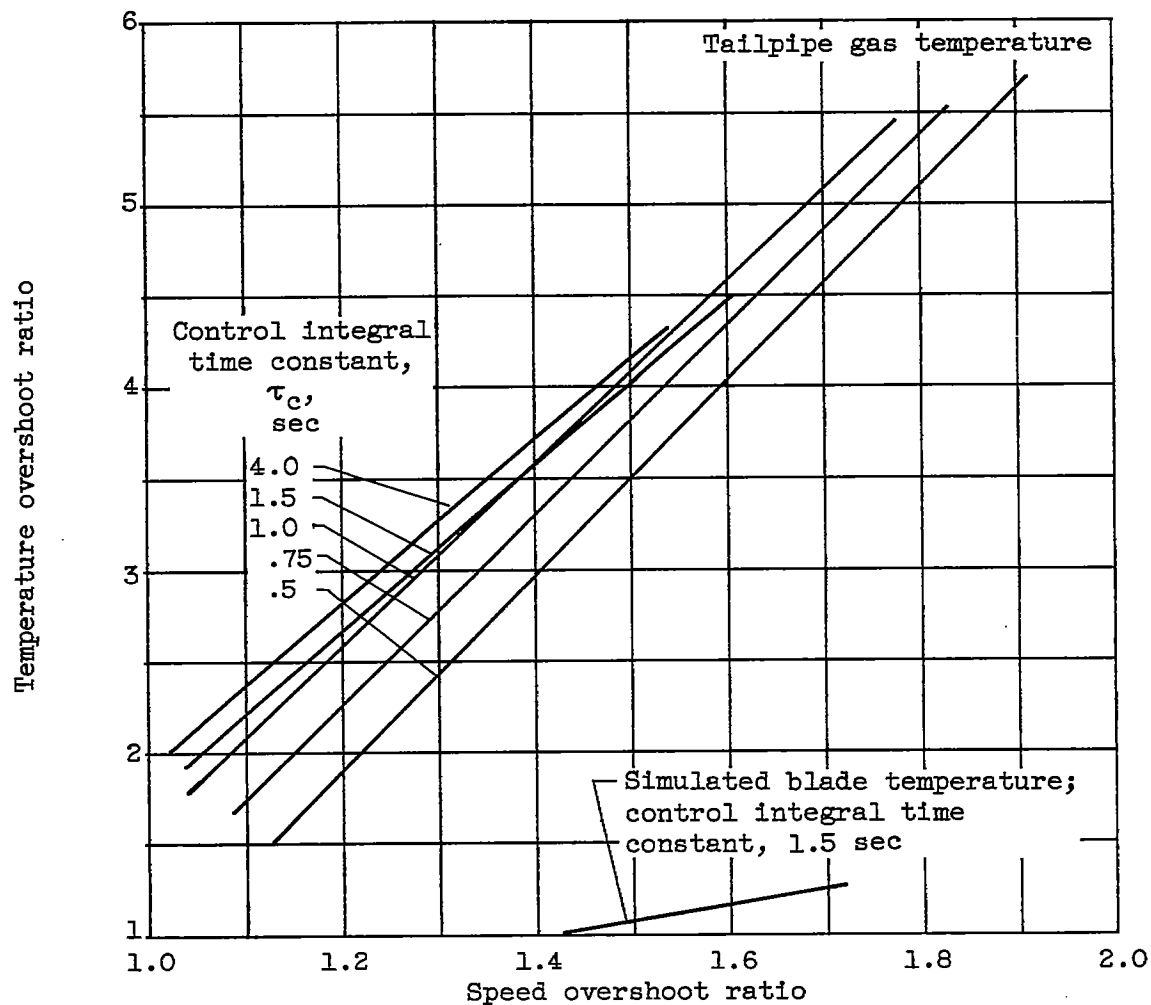


Figure 12. - Variation of tailpipe-gas-temperature overshoot ratio with speed overshoot ratio for speed - fuel-flow control.

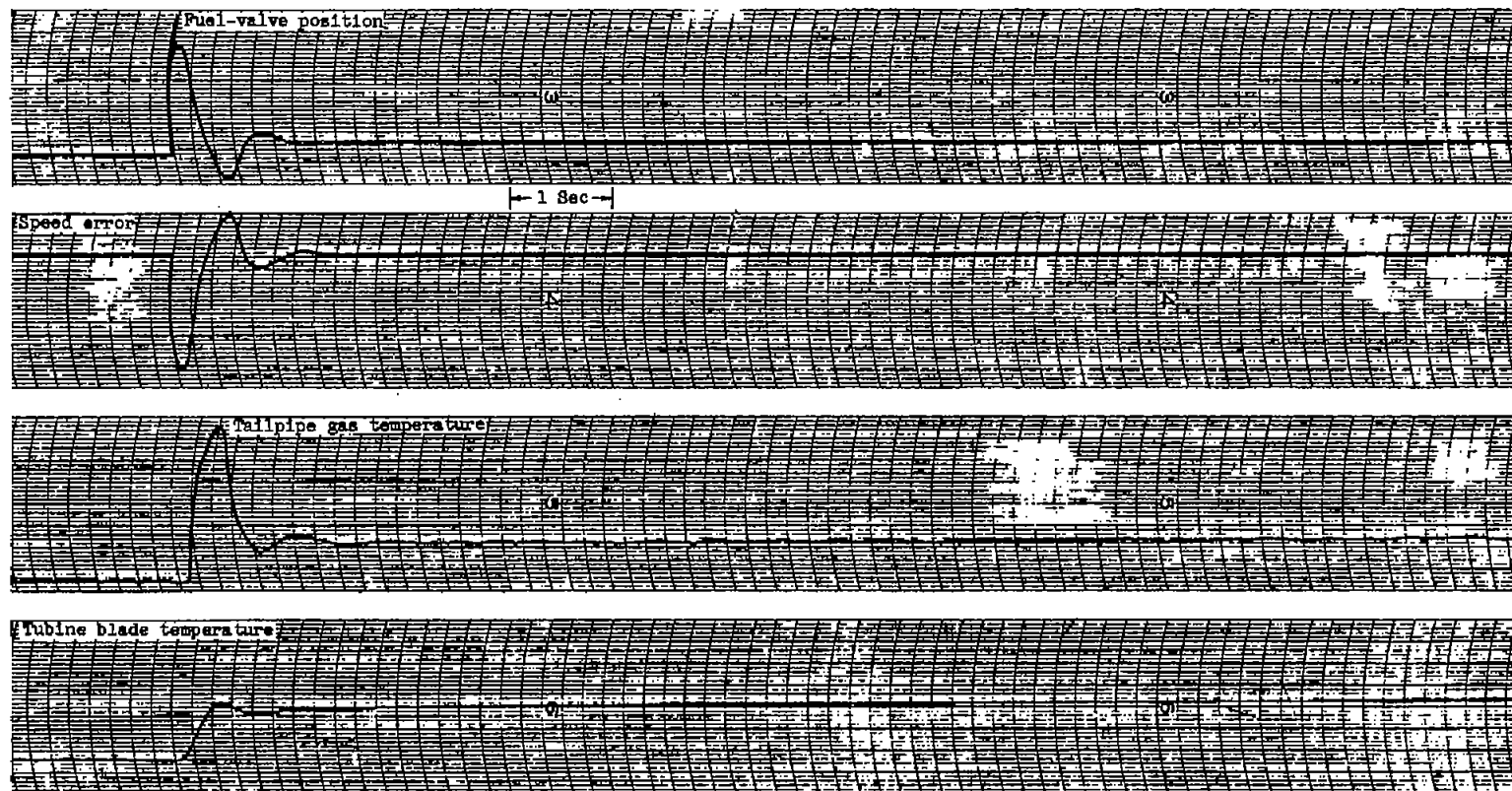
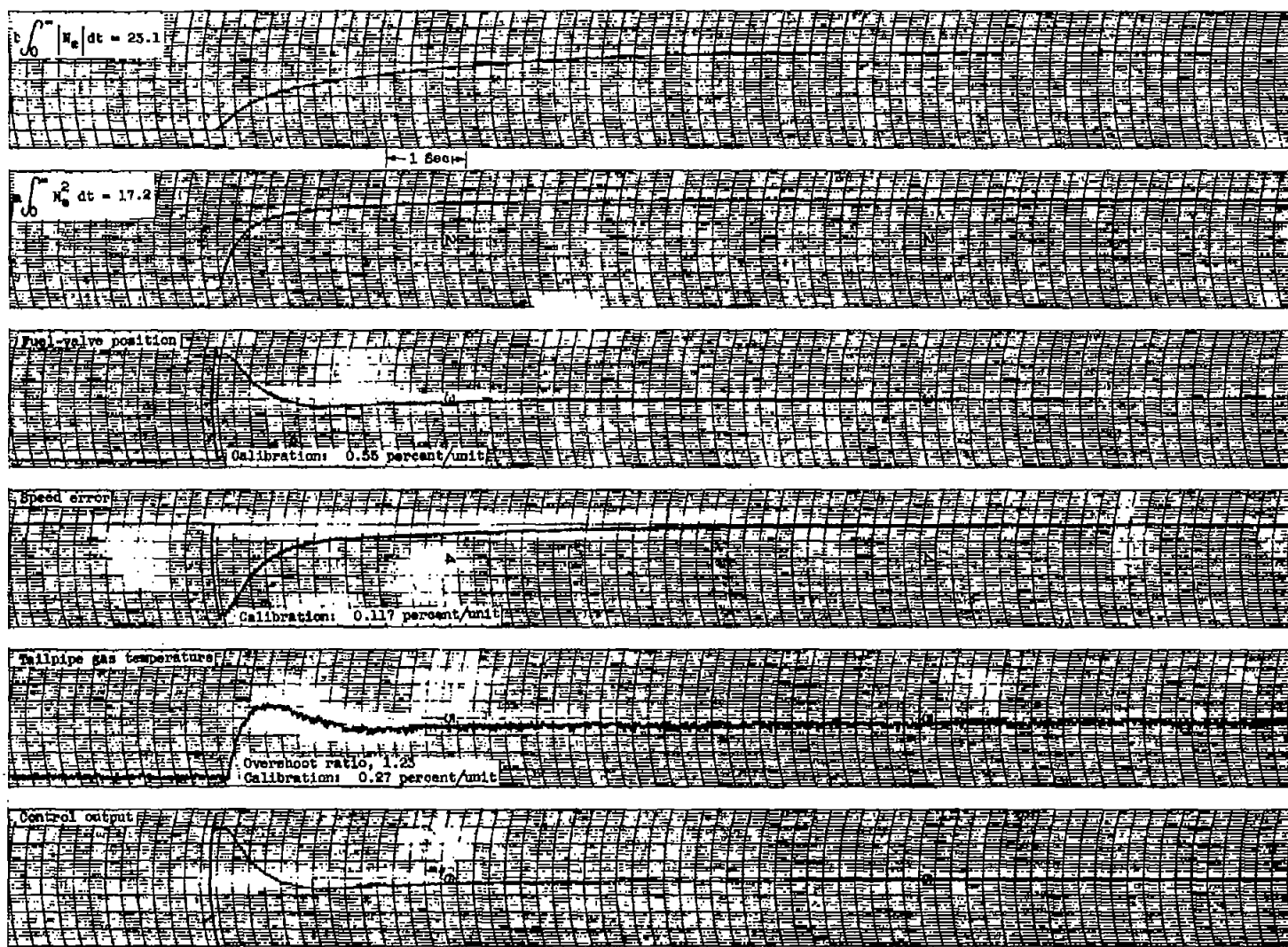
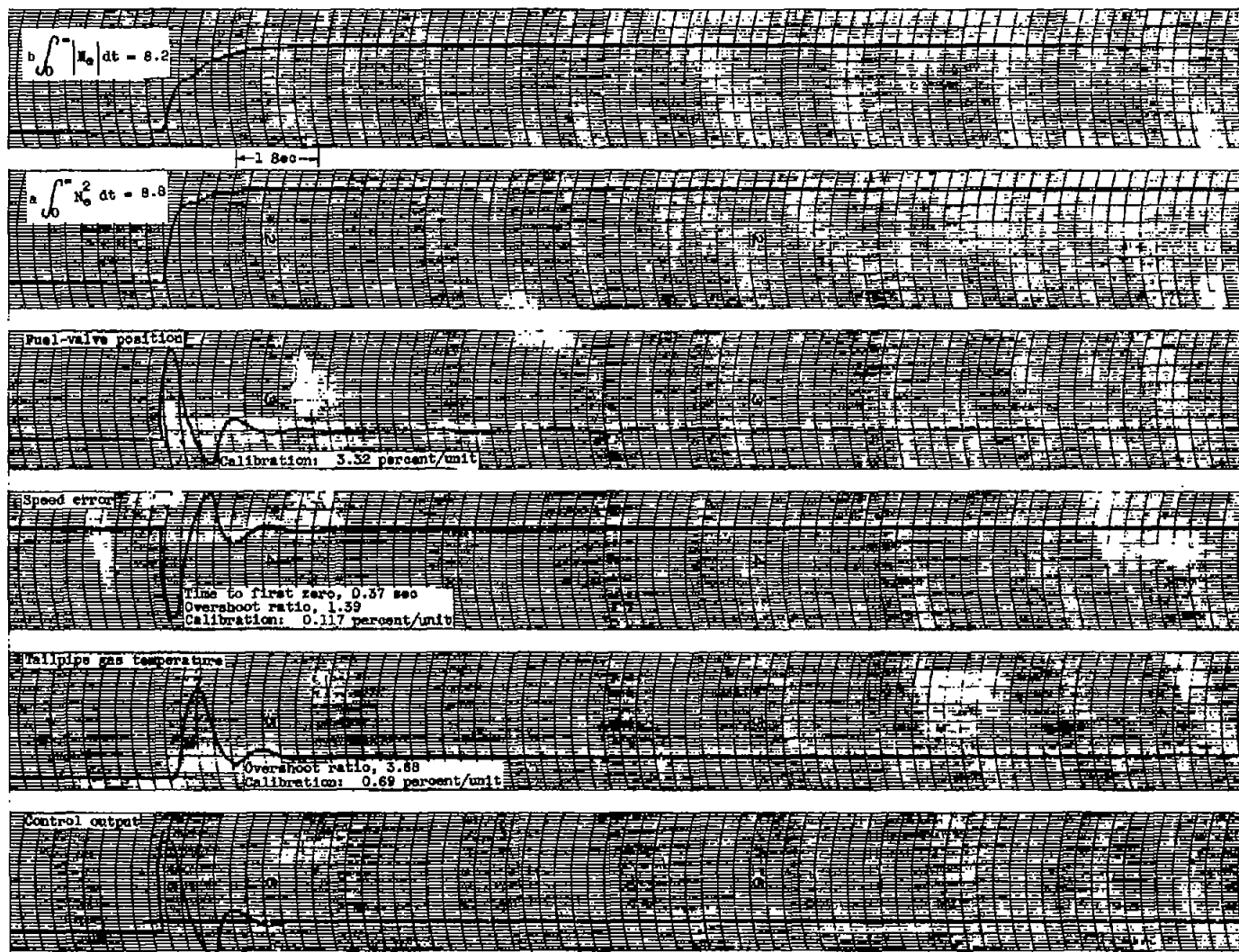


Figure 13. - Transient data for speed - fuel-flow control for step increase in engine set speed showing simulated turbine blade temperature. Control integral time constant, 1.5 seconds; loop gain, 7.4.



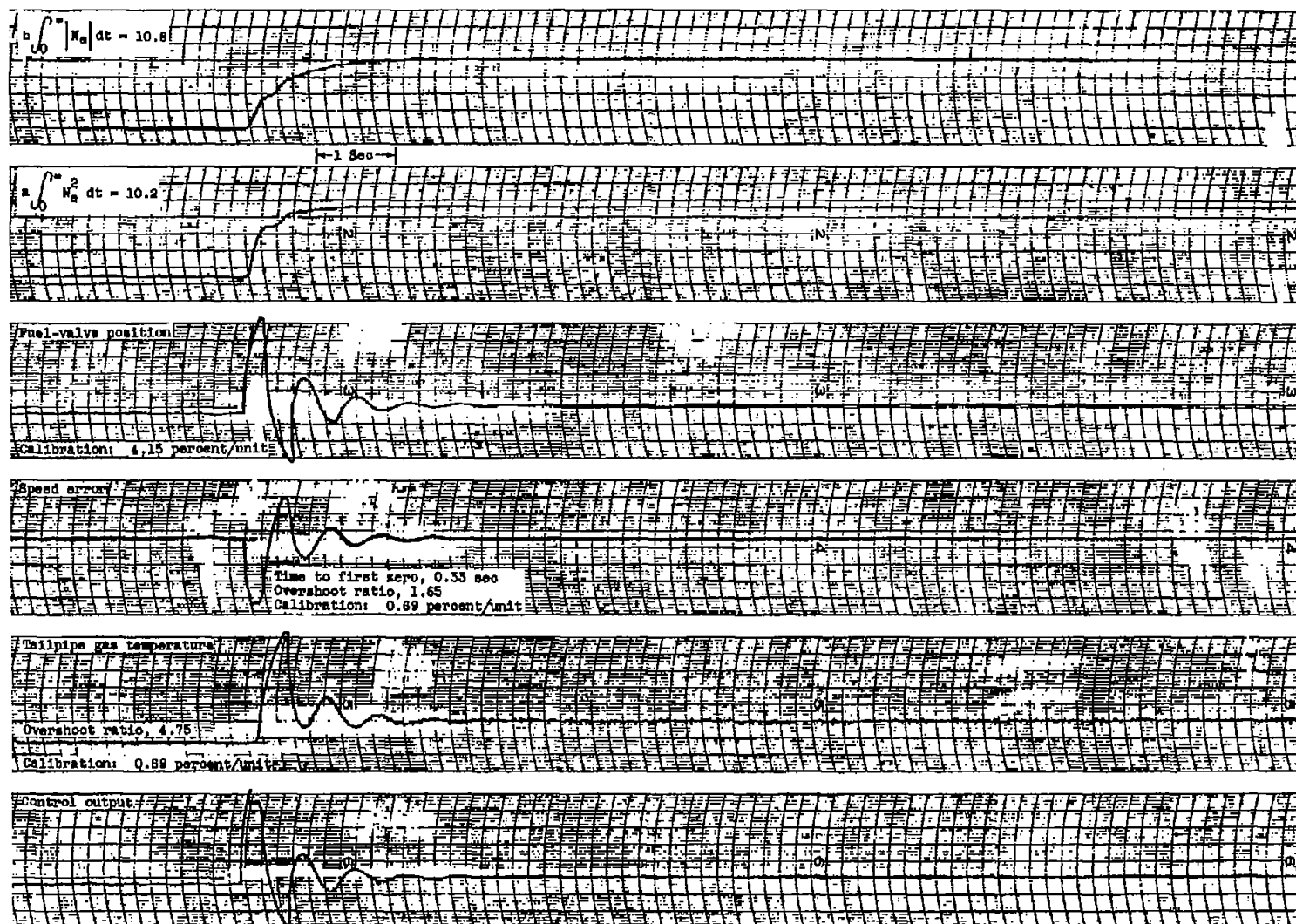
(a) Control integral time constant, 2.0 seconds; loop gain, 1.5.

Figure 14. - Transient data for speed - fuel-flow control with limited rate of change of fuel valve for step increase in engine set speed.



(b) Control integral time constant, 2.0 seconds; loop gain, 7.4.

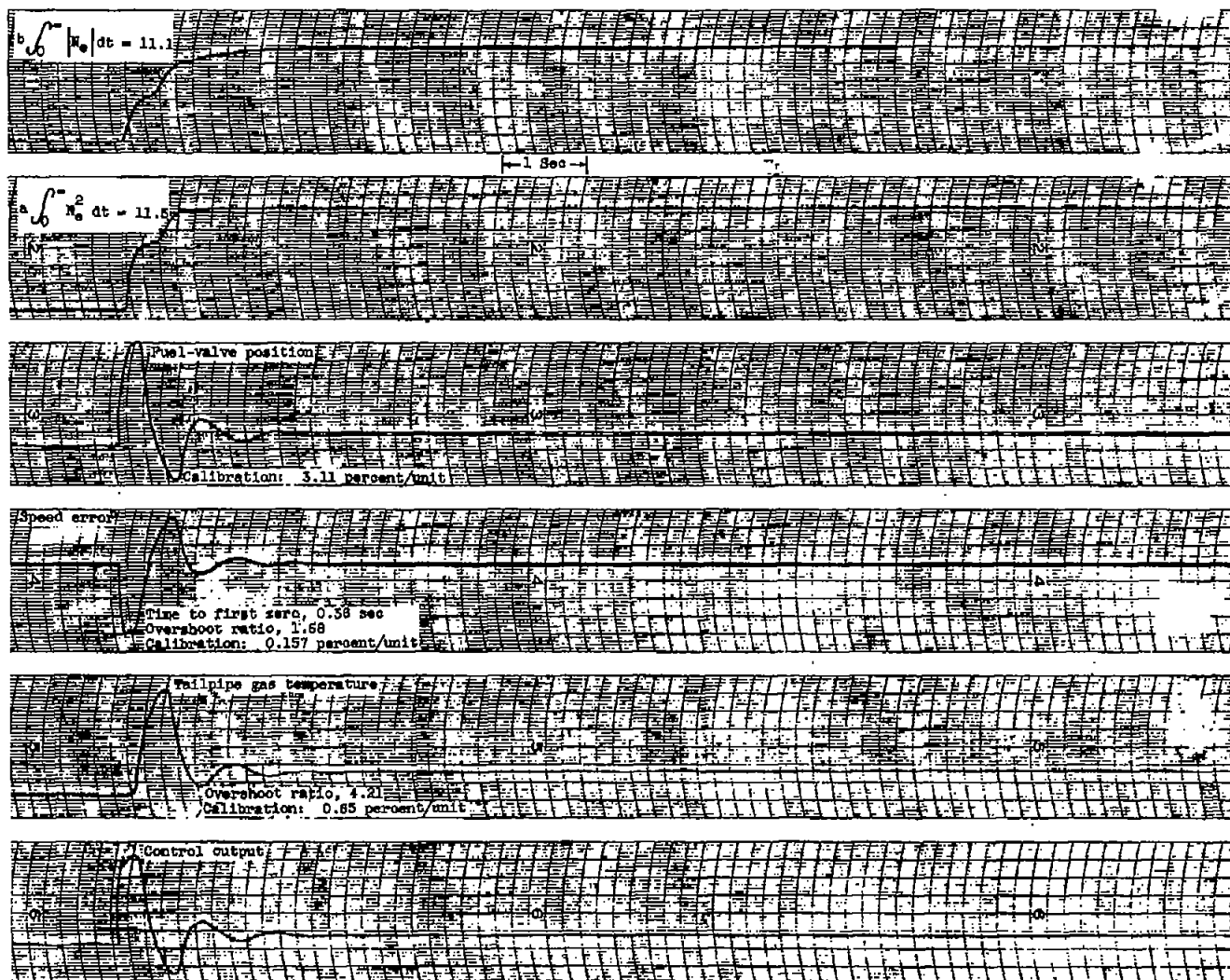
Figure 14. - Continued. Transient data for speed - fuel-flow control with limited rate of change of fuel valve for step increase in engine set speed.



(c) Control integral time constant, 2.0 seconds; loop gain, 10.5.

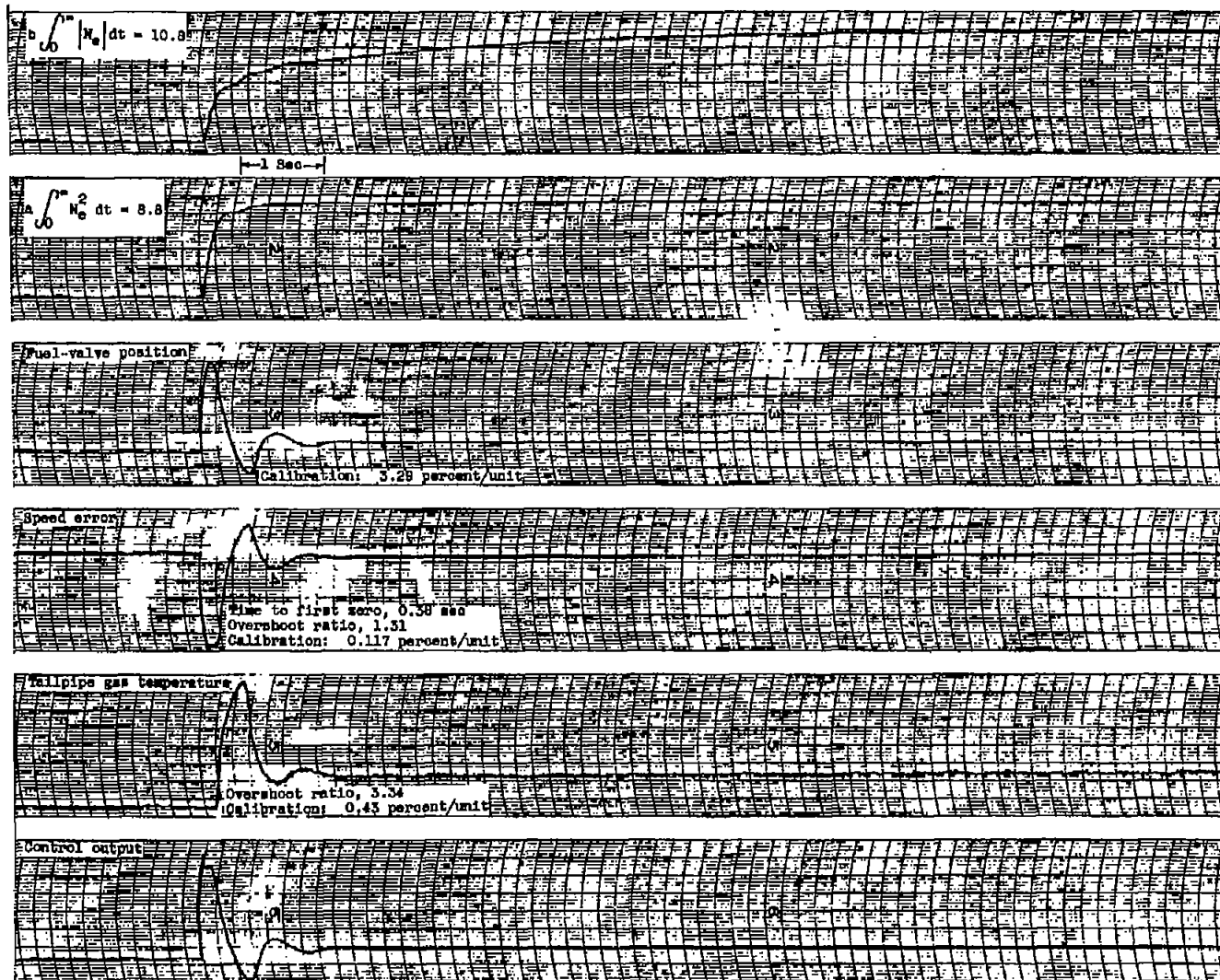
Figure 14. - Continued. Transient data for speed - fuel-flow control with limited rate of change of fuel valve for step increase in engine set speed.





(d) Control integral time constant, 0.5 second; loop gain, 7.4.

Figure 14. - Continued. Transient data for speed - fuel-flow control with limited rate of change of fuel valve for step increase in engine set speed.



(e) Control integral time constant, 4.0 seconds; loop gain, 7.4.

Figure 14. - Concluded. Transient data for speed - fuel-flow control with limited rate of change of fuel valve for step increase in engine set speed.

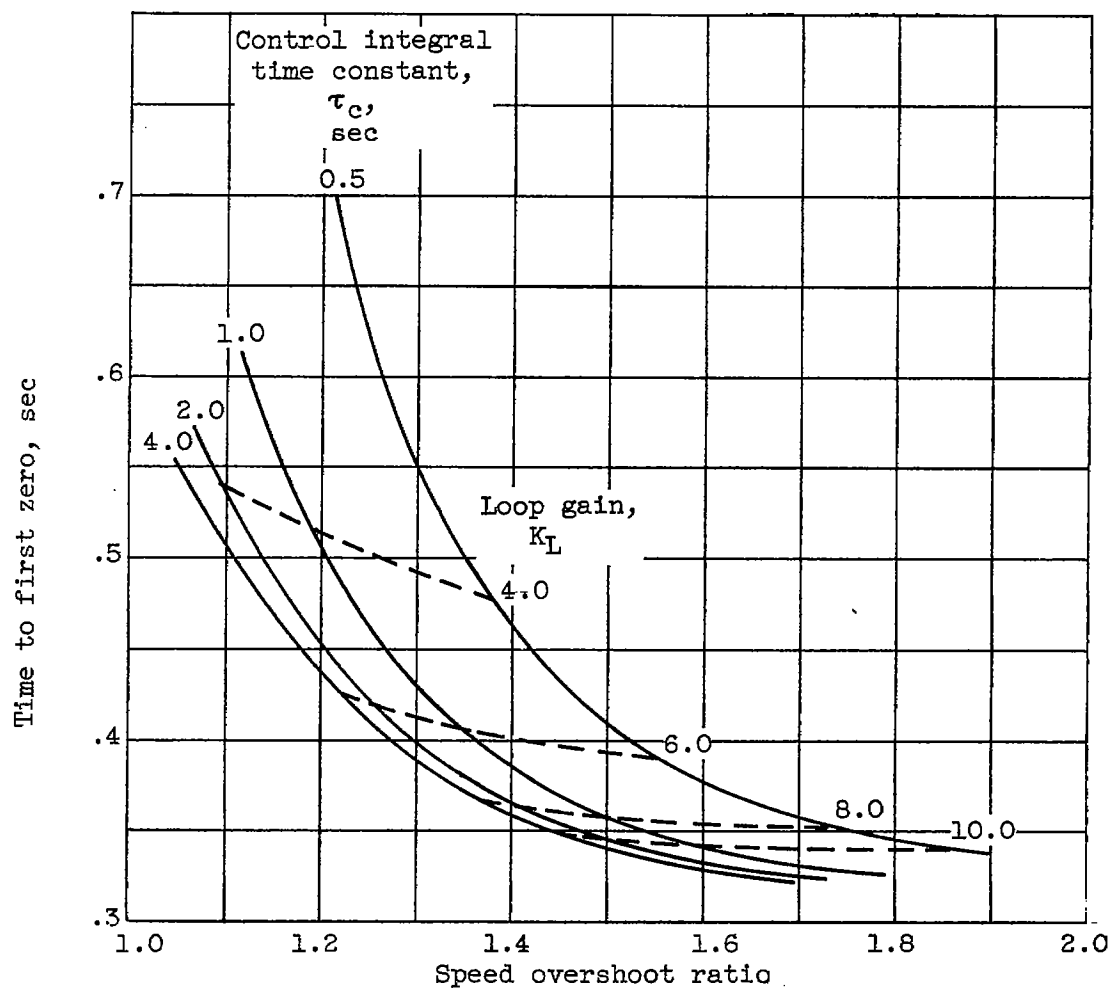


Figure 15. - Variation of speed overshoot ratio with time to first zero for speed - fuel-flow control with limited rate of change of fuel valve.

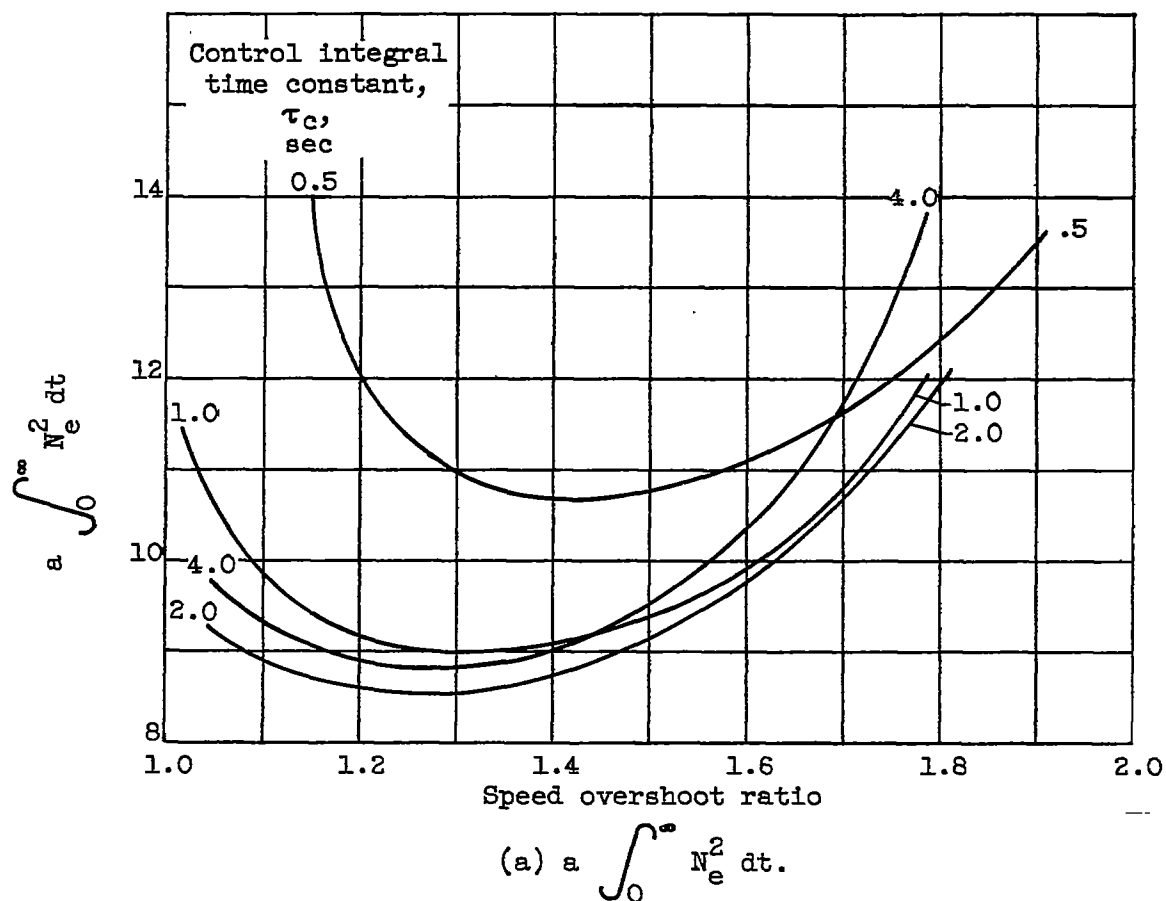


Figure 16. - Variation of integral criteria with speed overshoot ratio for speed - fuel-flow control with limited rate of change of fuel valve.

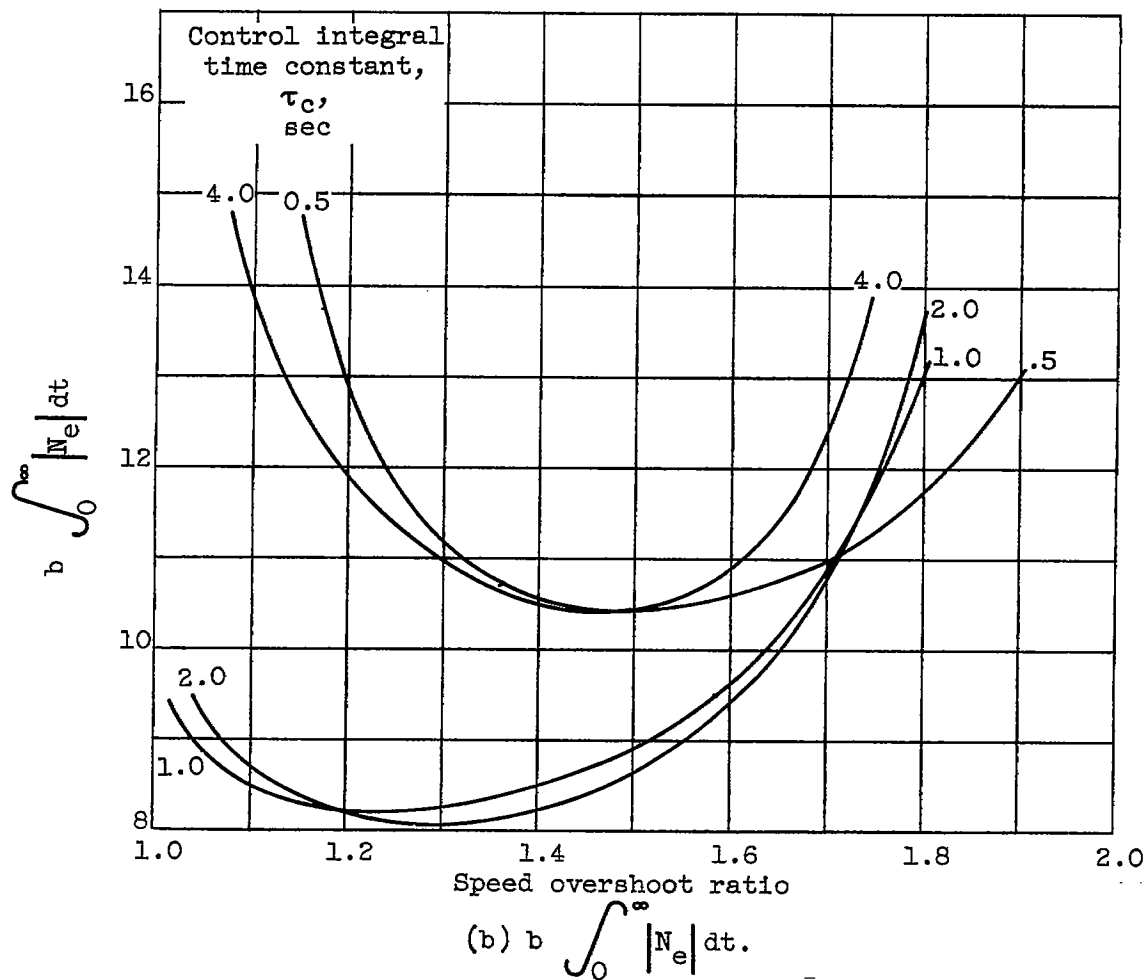


Figure 16. - Concluded. Variation of integral criteria with speed overshoot ratio for speed - fuel-flow control with limited rate of change of fuel valve.

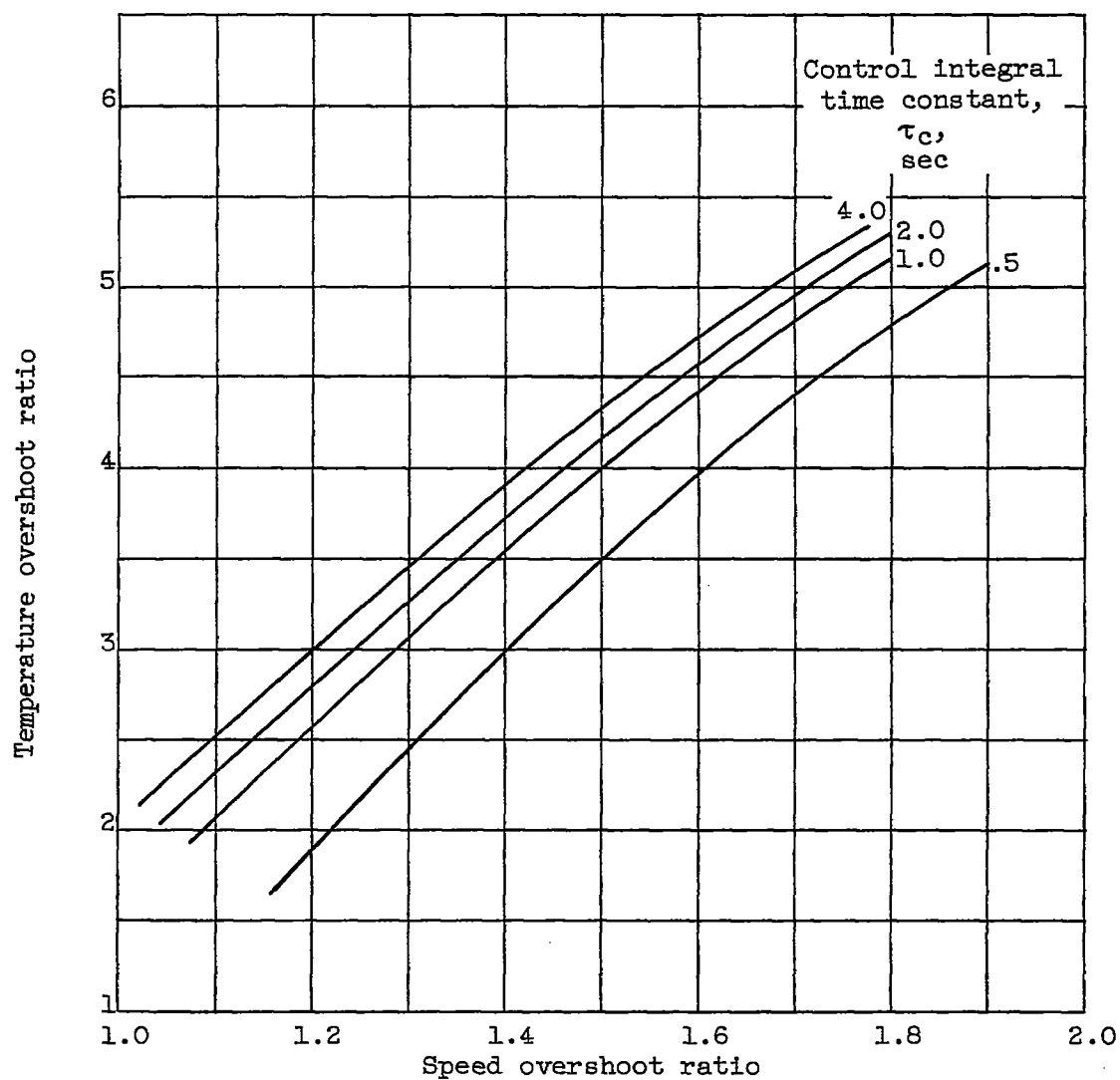
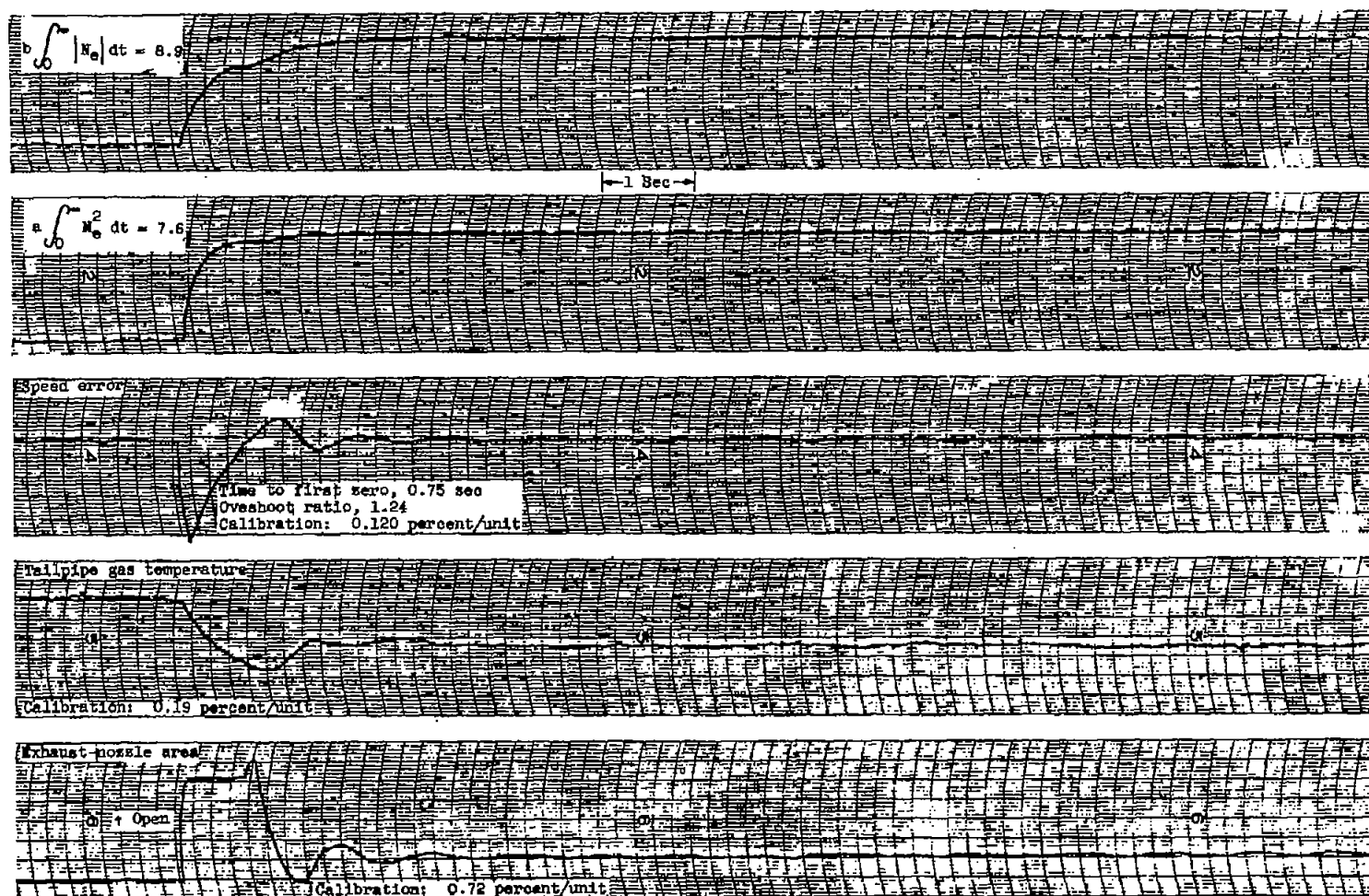
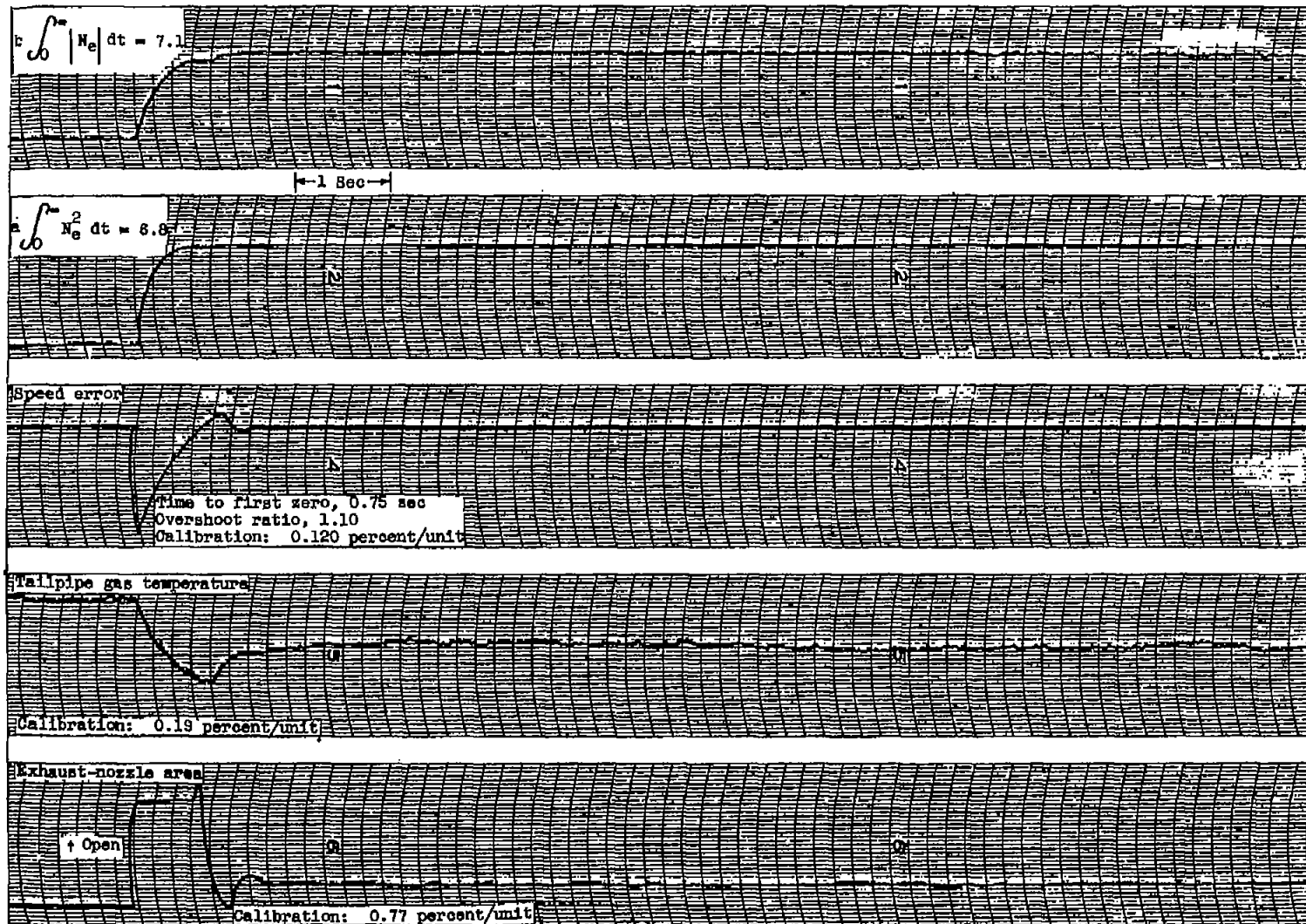


Figure 17. - Variation of tailpipe-gas-temperature overshoot ratio with speed overshoot ratio for speed - fuel-flow control with limited rate of change of fuel valve.



(a) Control integral time constant, 0.1 second; loop gain, 7.5.

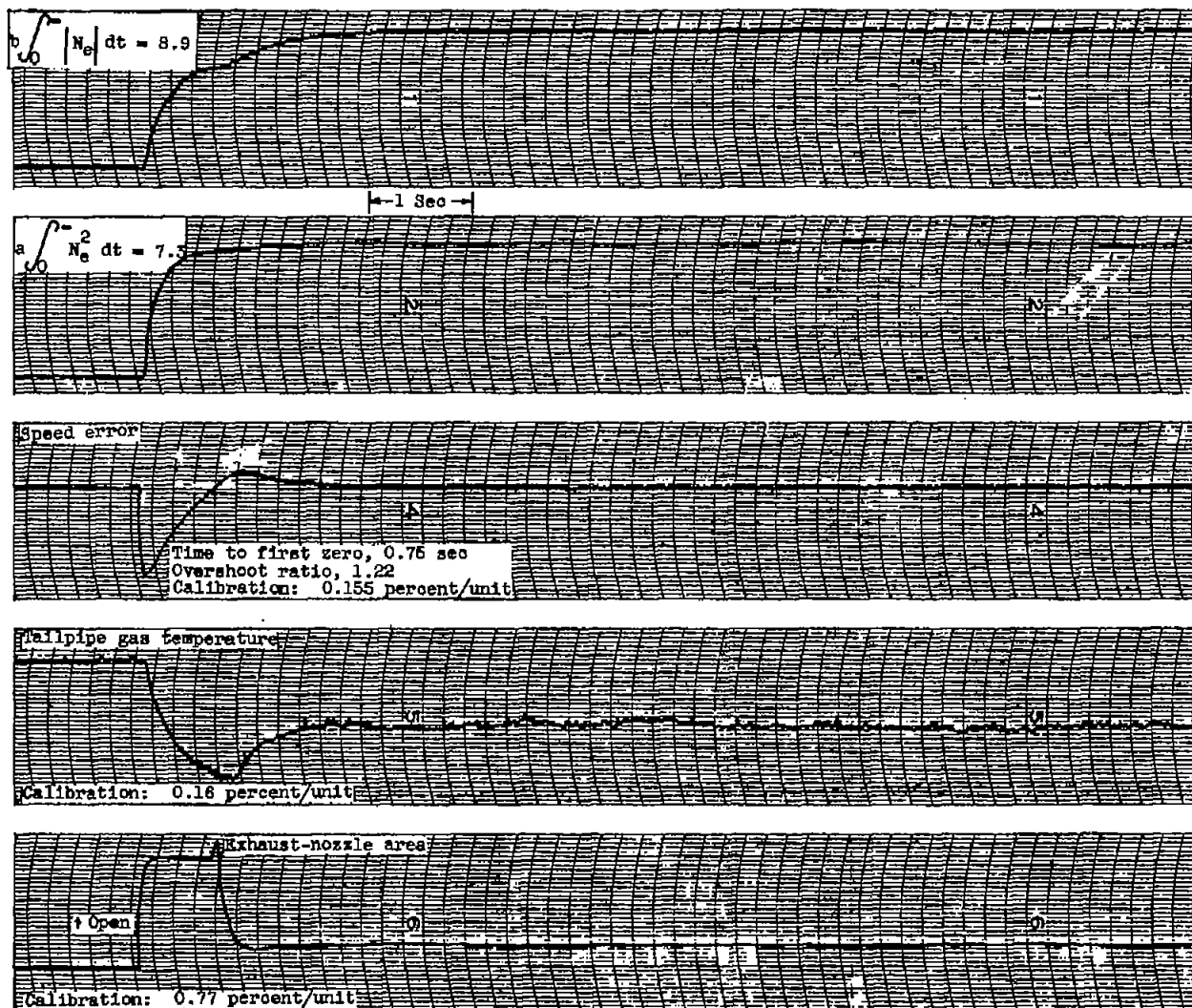
Figure 18. - Transient data for speed-area control type I for step increase in engine set speed.



(b) Control integral time constant, 0.1 second; loop gain, 17.5.

Figure 18. - Continued. Transient data for speed-area control type I for step increase in engine set speed.





(e) Control integral time constant, 0.5 second; loop gain, 17.5.

Figure 18. - Concluded. Transient data for speed-area control type I for step increase in engine set speed.

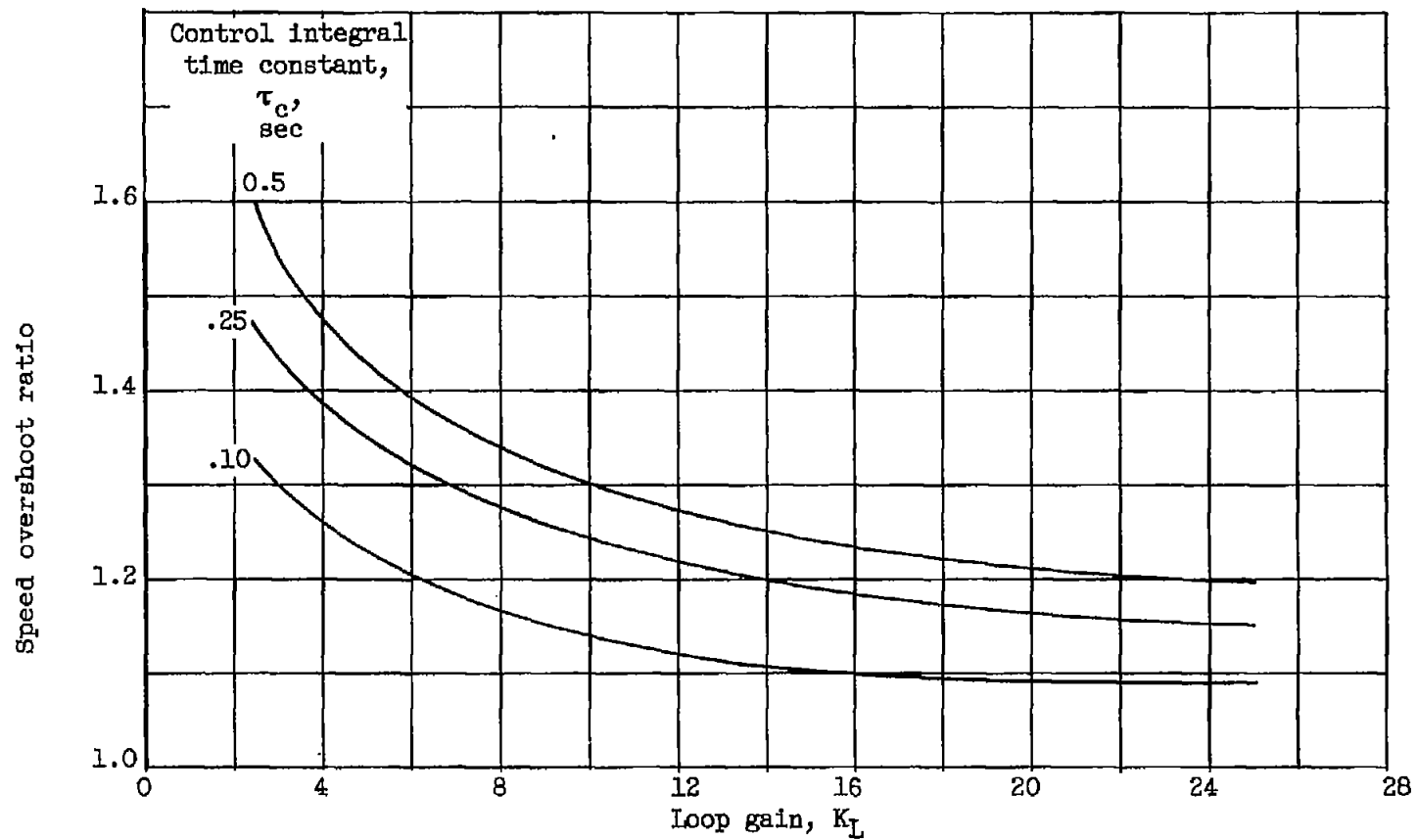


Figure 19. - Variation of speed overshoot ratio with loop gain for speed-area control type I.

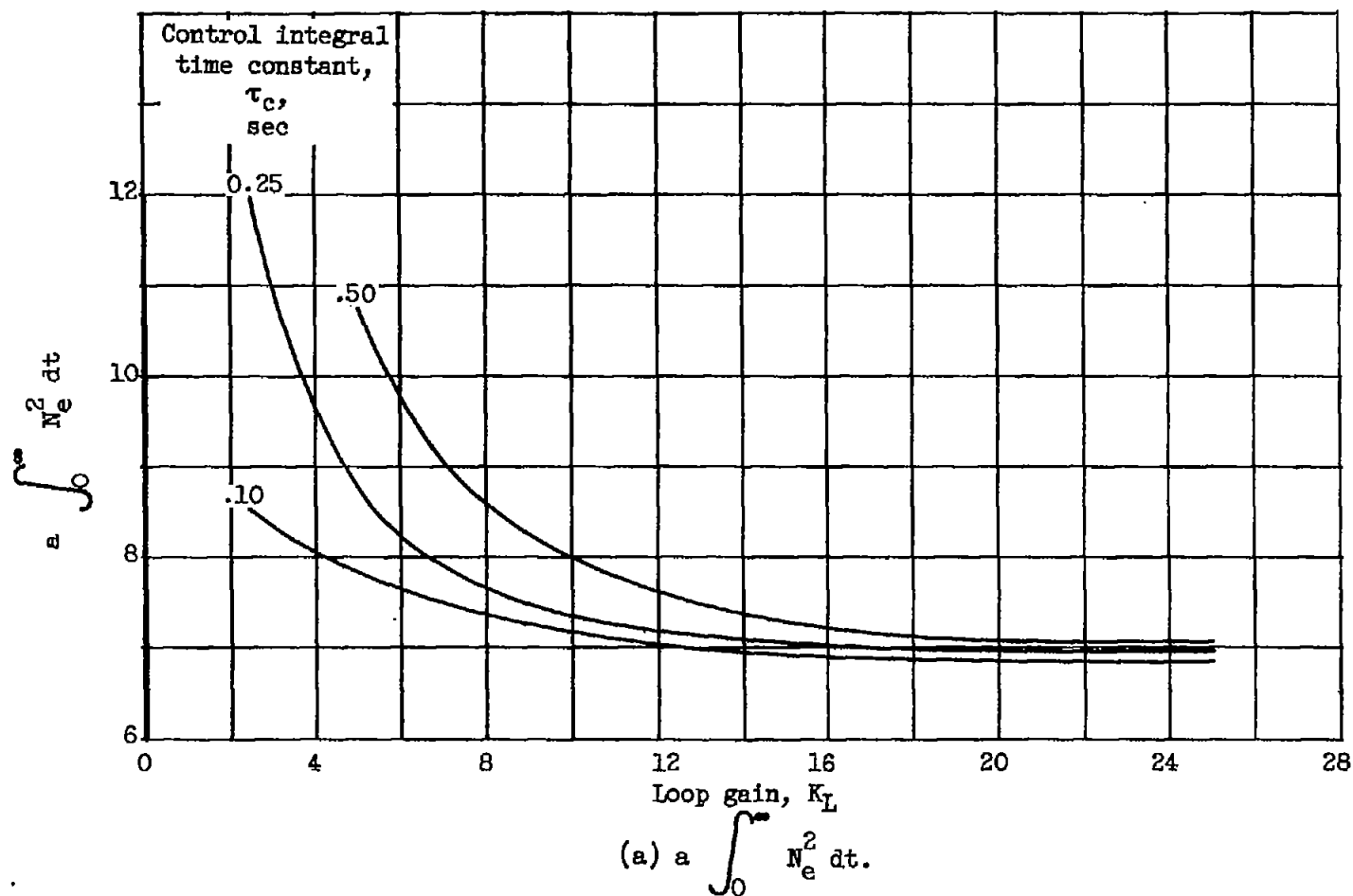


Figure 20. - Variation of integral criteria with loop gain for speed-area control type I.

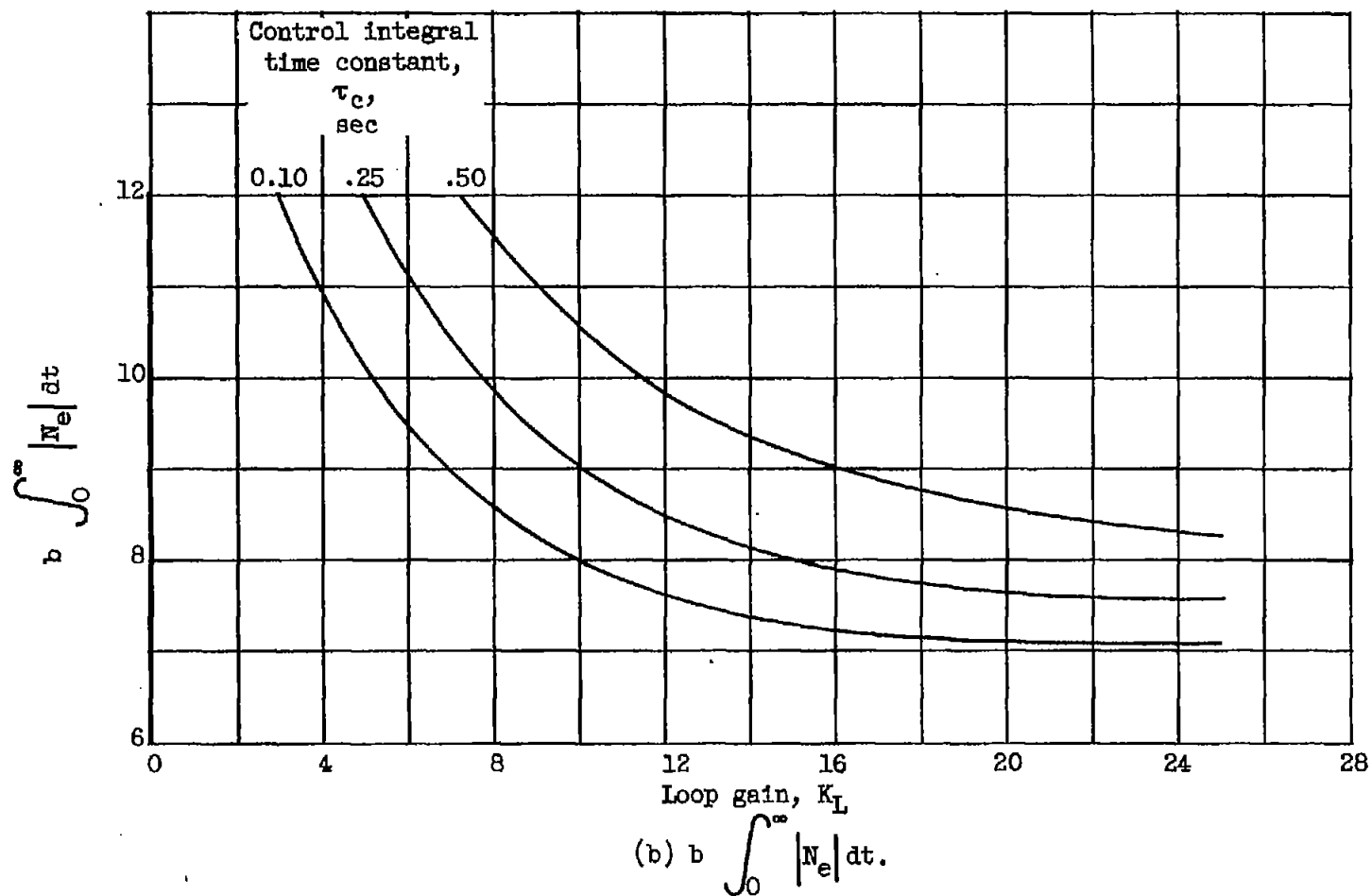
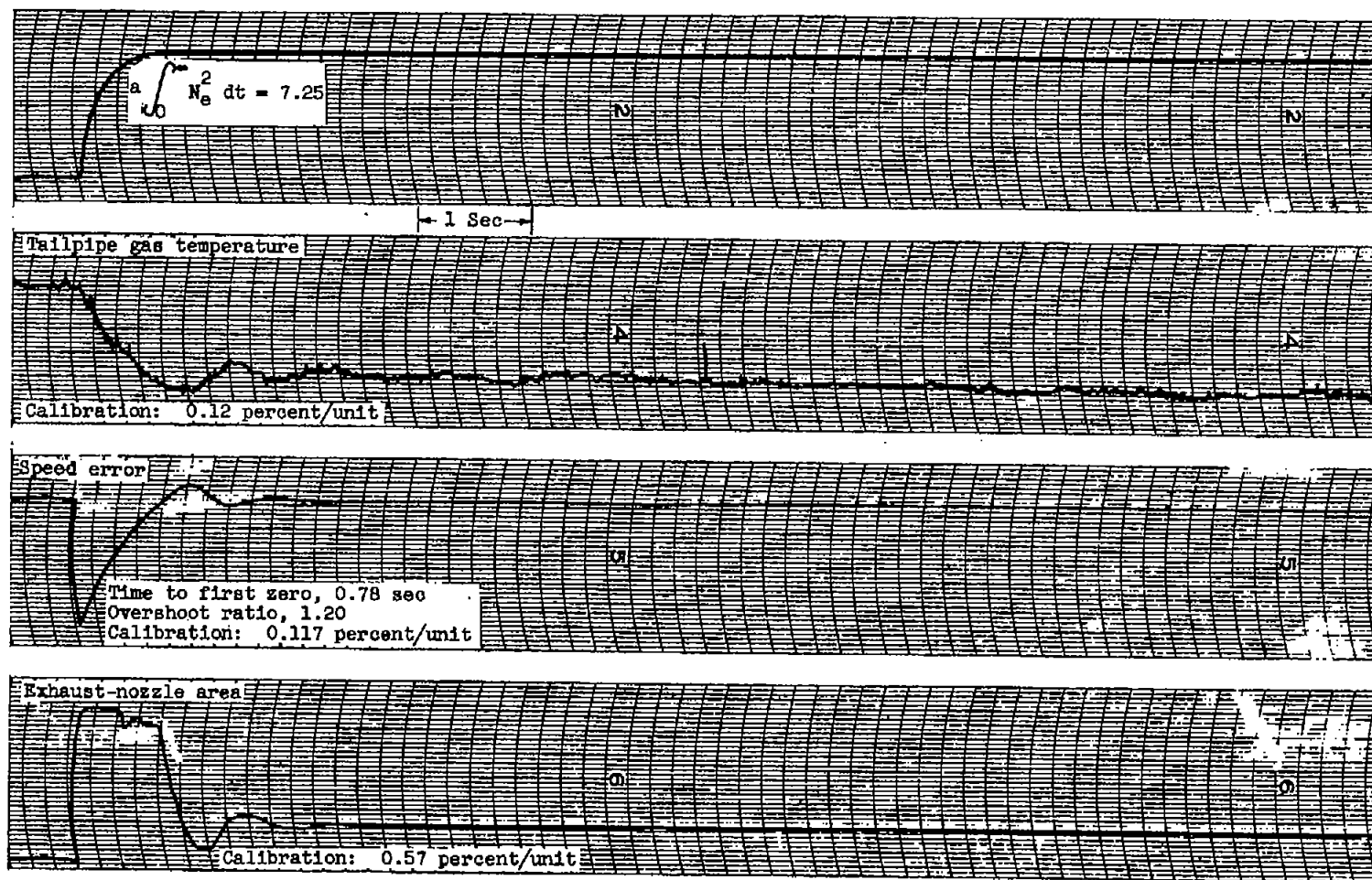
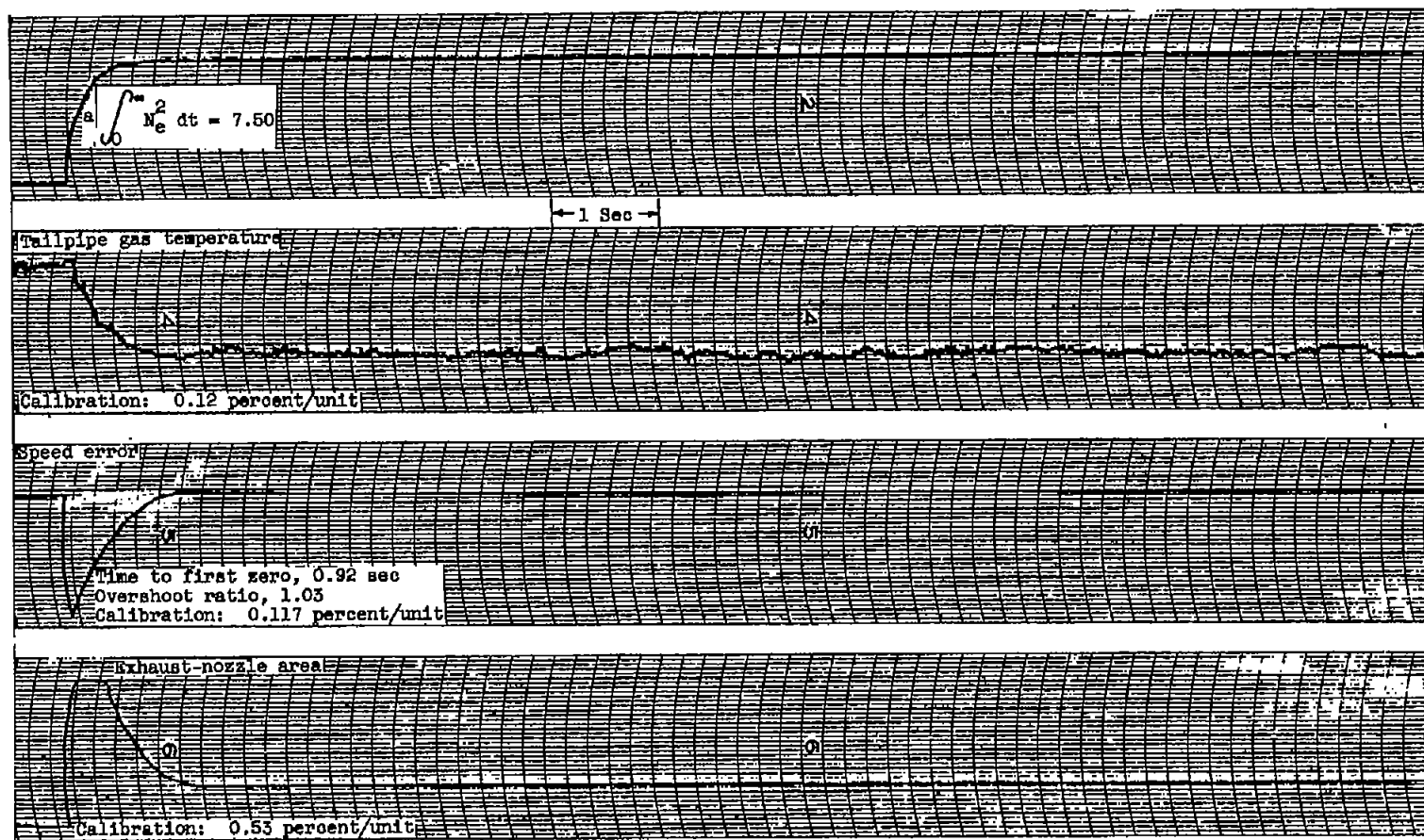


Figure 20. - Concluded. Variation of integral criteria with loop gain for speed-area control type I.



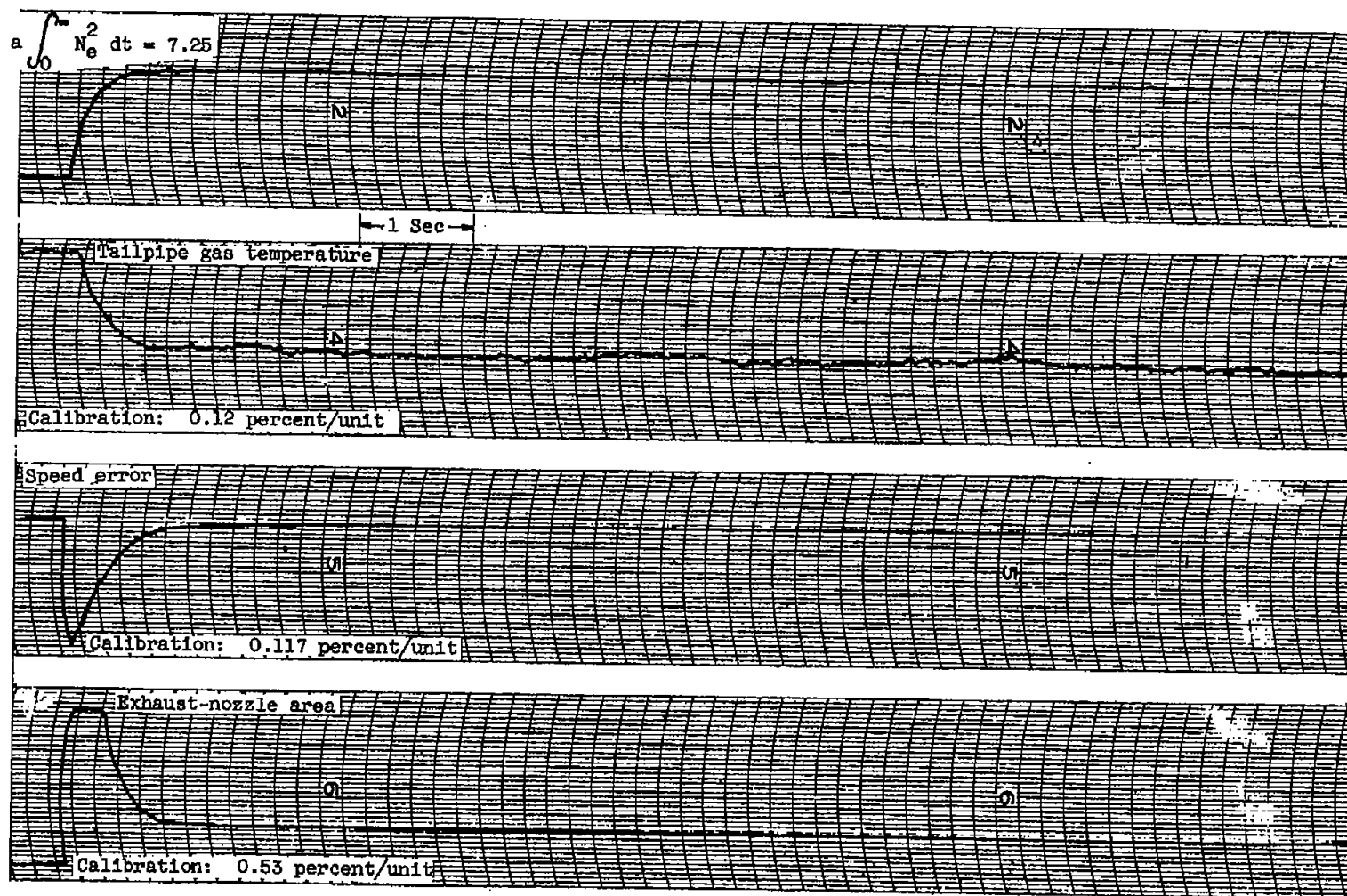
(a) Control integral time constant, 0.1 second; loop gain, 7.5.

Figure 21. - Transient data for speed-area control type II for step increase in engine set speed.



(b) Control integral time constant, 0.5 second; loop gain, 7.5.

Figure 21. - Continued. Transient data for speed-area control type II for step increase in engine set speed.



(c) Control integral time constant, 1.0 second; loop gain, 7.5.

Figure 21. - Concluded. Transient data for speed-area control type II for step increase in engine set speed.

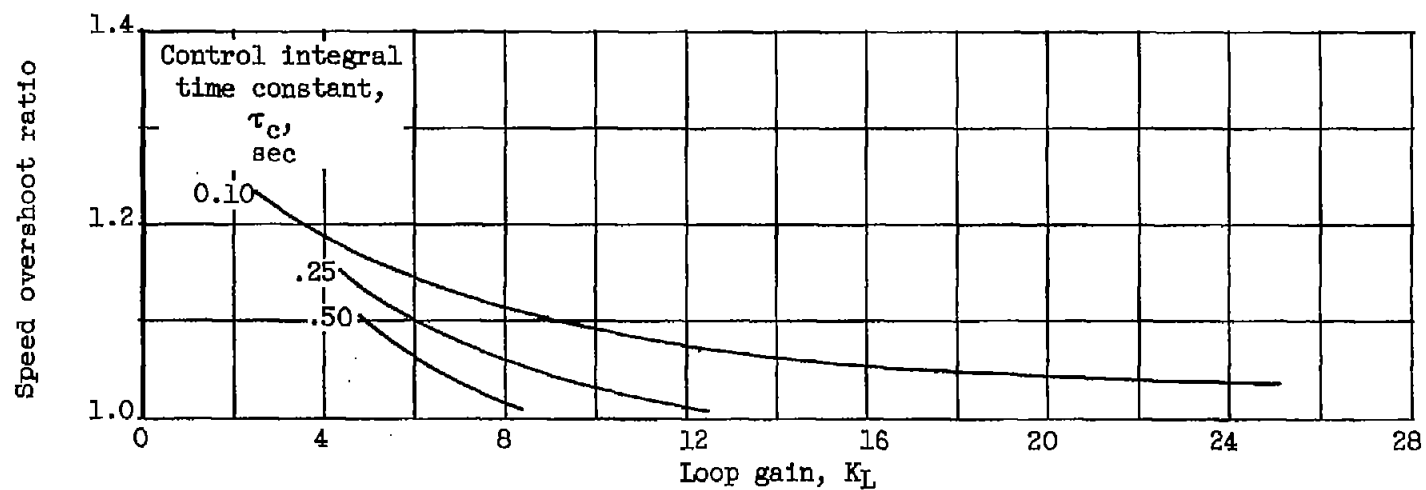


Figure 22. - Variation of speed overshoot ratio with loop gain for speed-area control type II.



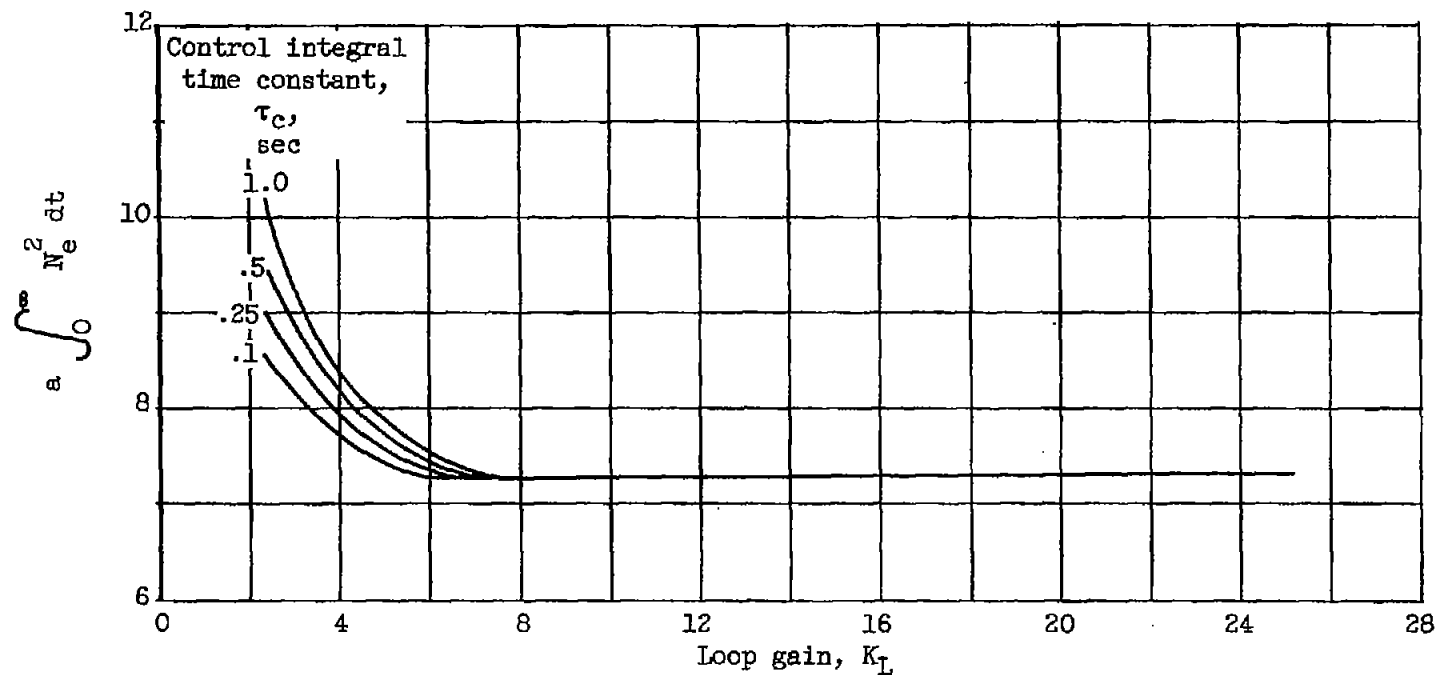


Figure 23. - Variation of integral criterion  $a \int_0^\infty N_e^2 dt$  with loop gain for speed-area control type II.